The adiabatic molecule–metal surface interaction: Theoretical approaches

G. P. Brivio

Istituto Nazionale di Fisica della Materia and Dipartimento di Scienza dei Materiali, Università di Milano, 20126 Milano, Italy
and Dipartimento di Fisica, Università di Milano, 20133 Milano, Italy

M. I. Trioni

Istituto Nazionale di Fisica della Materia and Dipartimento di Fisica, Università di Modena, 41100 Modena, Italy
and Dipartimento di Scienza dei Materiali, Università di Milano, 20126 Milano, Italy

Ab initio methods for calculating the adiabatic electronic properties of a single isolated molecule interacting with a metal surface are reviewed. First the fundamental approaches of Anderson, Grimley, and Newns for chemisorption, as well as of Zaremba and Kohn, for physisorption, are outlined. Then the density-functional theory and its approximations are considered. The different models for the adsorbate system are described. They comprise those in which the system has a finite volume—i.e., the cluster, the slab, and the supercell models—and those which take into account the semi-infinite nature of the substrate—i.e., the embedding approach based either on the Dyson equation or on Green's-function matching. Those definitions are also introduced that we deem important for the understanding of the physical properties of systems to be presented in this article. The lack of full screening in a localized region around the adsorbate, and hence the existence of long-range Friedel's oscillations induced by the adsorbate in the metal, are discussed. The way in which the lack of full screening influences the calculated adsorption energies is estimated by the grand-canonical functional. Recent *ab initio* results on physisorption of a noble-gas atom on metals deal mainly with the limits of validity of the simpler effective-medium theory and with the anticorrugating effect of He. Atomic chemisorption is considered in order to deal with the concept of bonding at a metal. Dissociative chemisorption calculations mainly treat the H_2 metal system. Here both the adiabatic electronic properties and the sticking probabilities recently obtained using the *ab initio* potential-energy surfaces are analyzed. Carbon monoxide chemisorption, lateral interactions between adsorbates, adatom diffusion, and chemisorption on stepped surfaces are presented as prototypes of the large variety of *ab initio* results currently available. Finally, the conclusions are devoted to the respective merits of the different theoretical approaches and to some future directions. [S0034-6861(99)00501-2]

CONTENTS

I. INTRODUCTION

Progress in microscopic experiments studying molecules on surfaces has given much impetus to theoretical research on the statics and dynamics of molecule-surface interaction. The static properties of interest comprise the geometrical configuration of the system, including possible reconstruction of the surface, the electronic structure of the system, its adiabatic potential-energy surfaces, its vibrational properties, and intermolecular interactions. The dynamic time-dependent processes to be studied include sticking, desorption, and diffusion on the surface. Reactions can occur on the surface and are also of interest; a simple example is dissociative sticking, where the molecule is separated into fragments when it

binds on a surface; the inverse process is called associative desorption (Lundqvist, 1984; Gomer, 1990; Brivio and Grimley, 1993). The binding of a molecule[1] to a surface is called chemisorption if the bond involves significant sharing of electrons beween the molecule and the solid, physisorption if the bond is the weaker van der Waals interaction, and adsorption in general. For example, the noble gases bind to surfaces by physisorption.

In this article we shall focus our attention on molecule-surface systems in which the substrate is a metal. In fact, a complete description of the molecule-metal interaction, including both the statics and the dynamics, would provide an understanding of several phenomena of fundamental importance in surface science. These include heterogeneous catalysis, corrosion, and the growth of thin films (Sinfelt, 1984; Hamnett, 1990). Although important processes such as catalysis are more efficient on polycrystalline surfaces, the fundamental properties of the interactions are easier to study, both experimentally and theoretically, on single-crystal surfaces. So, owing to the more fundamental character of the measured or calculated results obtained on a single-crystal surface, the information gained about the basic interactions can then be applied to understand the main trends for surface phenomena on more complex structures (Langmuir, 1922; Ertl, 1994). Only very recently have studies of the molecule-metal interaction on stepped surfaces been undertaken (Feibelman, 1992a; Wang and Ehrlich, 1993; Stumpf and Scheffler, 1996).

One of the main aims of theory in surface science is to describe in microscopic detail the chemical transformations associated with heterogeneous catalysis. At present we are still far from being able to follow all steps of a heterogeneous catalysis reaction on a single-crystal surface by solving a classical or a quantum-mechanical equation of motion. But it is feasible to study more elemental processes related to catalysis for adsorbates which are reactants, products, or intermediates. For example, there is general consensus that ammonia synthesis is controlled on Fe(111) by the nitrogen dissociative sticking coefficient (probability) (Grunze, 1982). So the microscopic description of a more elemental surface process, e.g., the sticking of nitrogen, could provide the correct input for more complex phenomena.

Consider now a process such as scattering, sticking, or desorption of a molecule on a metal, which clearly requires the solution of a time-dependent equation. Before such a calculation can be performed one needs to know the potential-energy surfaces and the couplings to excitations as well (Brivio and Grimley, 1993). At the least, the ground-state adiabatic potential-energy surfaces of the molecule-metal interaction (statics of adsorption) are needed as the input for a dynamical calculation. Such potential-energy surfaces (Darling and Holloway, 1995) have to be known in great detail, since the presence or absence of even a shallow activation barrier in the molecule-surface potential modifies drastically the physics of the problem. For example, observe that, for an initial molecule kinetic energy smaller than 100 meV, the dissociative sticking probability of H_2 on Ni(110) behaves very differently from that on Ni(111), the latter being significantly lower due to the presence of an activation barrier of about 0.1 eV (Robota *et al.*, 1985; Rendulic, Anger, and Winker, 1989; Yang and Whitten, 1993). The statics of adsorption can also by itself provide important information. The electronic spectrum can be measured by photoemission experiments, and is affected by an adsorbate on a metal surface. It can tell us whether the bond is ionic or covalent, which electronic orbitals are involved, and any hybridization effect. Recently, as will be discussed later, a new goal has been set forward in chemisorption theory, namely, to obtain the general trends of the bond of a particular molecule on several surfaces on the basis of the substrate band properties alone (Hammer, Morikawa, and Nørskov, 1996).

It is therefore desirable that electronic adiabatic properties of the molecule-surface system be obtained with the greatest accuracy independent of any parametrization subordinate to a specific model. This fact was already recognized some twenty years ago by Grimley (1975), who wrote

> The goal of chemisorption [but say more generally of the statics of adsorption] theory is to determine for any adsorbent/adsorbate system the equilibrium positions of all nuclei, the ground-state energy, the elementary excitations, and the responses to external probes using only the value of the fundamental constants, e, m_e, $\hbar$, and ϵ_0 (the permittivity of free space).

This sentence explains the ultimate aim of any electronically adiabatic molecule–surface theory, giving a clear definition of a first-principles or *ab initio* method. Of course such a goal is still unattained. However, with the help of the numerical techniques now available thanks to a great increase of the computational power, it is possible to study several properties of the adiabatic molecule–metal interaction from first principles for many simple systems which might be prototypes for more complex ones. Although limitations, to be discussed in this article, still exist, one can now try to work out a parameter-free calculation both to reproduce the experimental results and to obtain new ones. For this reason, our article will deal mostly with the adiabatic properties of the molecule-metal interaction obtained by *ab initio* approaches. More empirical models are often still necessary: at present, even for a simple phenomenon such as the interaction of a noble gas with a metal surface, no unified *ab initio* theory capable of computing the potential-energy surface exists over the full range of atom-surface distances (Sec. VI).

Following the Born-Oppenheimer adiabatic approximation (Born and Oppenheimer, 1927; Born and Huang, 1954), one usually tackles the many-electron problem at a fixed configuration of the molecule's nuclei

[1]In this article we use the word "molecule" to refer to both molecules and atoms.

with respect to the metal surface, while the lattice is kept rigid (Brivio and Grimley, 1977; Darling and Holloway, 1995).

Apart from the van der Waals interaction between a molecule and a metal surface (Secs. II, VI) one usually employs methods either based on the Hartree-Fock approach or, more and more frequently, on the density-functional formalism. In this latter framework, solutions to the effective one-electron equation are obtained in the local-density approximation, recently also including gradient corrections (Sec. III). When the density-functional formalism with its above-mentioned approximations is considered, one solves the Kohn-Sham (Kohn and Sham, 1965) equation either self-consistently or by the Car-Parrinello (Car and Parrinello, 1985) approach or similar methods, which calculate the ground-state adiabatic properties of the system by minimization procedures and may also let the substrate ions relax.

In our article we shall present the earlier theoretical approaches in Sec. II and the density-functional formalism that is currently used to treat the adiabatic molecule–metal interaction in Sec. III. Adsorption models and theoretical issues, such as the lack of full screening in the region where the electronic problem is solved, are then discussed (Secs. IV, V). Recent results for chemisorbed and physisorbed systems, which we deem to be important, will be described (Secs. VI, VII). We do not attempt a comprehensive review of the theoretical literature in this field. Instead we would like to emphasize two points, which are central to the statics of adsorption: the importance of the electron-electron interaction and hence of the Coulomb and exchange interactions and of correlation; and the particular symmetry of the system, which is different from either that of an impurity in a bulk with a periodic lattice structure or that of a molecule in vacuum. Different schemes have been devised to tackle the latter problem. Three of them are especially relevant here: the straightforward cluster approach, in which the molecule is coupled to a cluster of as many substrate atoms as possible (Sec. IV.A), the so-called embedded-adsorbate method (Sec. IV.B), which takes into account a single molecule interacting with a semi-infinite solid, and the slab and supercell methods (Sec. IV.C). In the two last methods one constructs a fictitious periodic lattice of either two or three dimensions, containing periodic units of a portion of the bulk plus the molecule. In all these approaches one solves an effective one-electron Schrödinger equation in a finite volume by projecting it onto a suitable basis set. Although one looks for a solution independent of the choice of the basis set and of the size of the above-mentioned volume, in practice long-range Friedel's oscillations in the bulk (Sec. V.B) and the correct behavior of the electronic wave function far from the surface cannot be taken into account exactly.

We begin our review by discussing in the next section the Anderson-Grimley-Newns model for chemisorption and the Zaremba and Kohn approach to physisorption, which are historically very important. In fact, they introduced treatments that account for important aspects of the electron-electron interaction in the statics of adsorption. In the subsequent sections all the above-mentioned points will be analyzed.

II. *AB INITIO* METHODS: MOTIVATIONS AND HISTORICAL BACKGROUND

In this section we shall try to review the main motivations for an *ab initio* theory of chemisorption and physisorption from an examination of the physics of such phenomena. We recall that in an *ab initio* calculation besides the fundamental constants (Grimley, 1975) one fixes only the distribution of the positive charge. Consequently, the theoretical methods for chemisorption and physisorption to be described in this section are not fully *ab initio*. However, they represent a first attempt in this direction and for this reason have greatly helped to advance work in this field.

We should also like to point out that in this review we shall concentrate on the theoretical treatments of an isolated (single) molecule interacting with a metal surface. This is because by this approach the fundamental properties of molecule-metal systems can be determined regardless of any interadsorbate lateral interaction, such as occurs for overlayers. Of course in this way the symmetry of the system under investigation is lowered. This explains why such theoretical studies have progressed more slowly than those of the electronic properties of full-coverage adsorbate overlayers. Slab/supercell calculations of molecule-metal systems, to be reviewed in this article, deal indeed with periodic overlayers of molecules. But in order to treat the single adsorbate molecule-metal interaction they aim at a very dilute overlayer limit.

A. The Anderson-Grimley-Newns model for chemisorption

Even though chemisorption and physisorption share common aspects, we shall deal with chemisorption first. Historically it was soon recognized that models based on the independent one-electron approximation, often in the tight-binding form, were inadequate (Grimley, 1958). Consider in fact a hydrogen (H) atom far from a transition-metal surface: the $1s$ orbital of H (ϕ_A), of energy $E_A=-13.6$ eV with respect to vacuum, is much below the Fermi energy of the metal, whose work function (for transition metals) is $\Phi\sim 4.5$ eV. So in the surface bond, electron transfer is expected to H. But if one electron is transferred, the $1s$ level is raised because of the Coulomb repulsion between the two electrons in ϕ_A. Such a Coulomb repulsion energy, which we call J_A, is fairly large, and it is usually taken as the difference between the ionization potential and the electron affinity of the unperturbed H atom, $J_A=12.9$ eV (Newns, 1969). Thus the chemisorbed system with two electrons on the hydrogen requires 3.8 eV to form. But, the observed chemisorption results in an energy gain of 3.5 eV rather than an energy cost.

On the other hand, by taking into account the repulsive Coulomb electron-electron interaction in the orbital

ϕ_A, we expect the energy E_A to be changed by chemisorption in the following way:

$$\epsilon_{A\sigma}=E_A+J_A\langle n_{A-\sigma}\rangle, \tag{1}$$

where $\langle n_{A\sigma}\rangle$ is the $1s$ orbital occupancy per spin σ ($\uparrow$ or $\downarrow$). Now Eq. (1) shows that the effective energy $\epsilon_{A\sigma}$ of the orbital ϕ_A in the adatom-metal system depends on its occupancy $\langle n_{A-\sigma}\rangle$ by an electron of opposite spin. Conversely, the occupancy $\langle n_{A-\sigma}\rangle$ depends on the relative distance in energy of $\epsilon_{A\sigma}$ from the Fermi level, so chemisorption theory has to determine $\epsilon_{A\pm\sigma}$ and $\langle n_{A\mp\sigma}\rangle$ in a self-consistent way. This shows that the electron-electron interaction is crucially important in the determination of these quantities (Grimley, 1975).

In order to extract the main trends of chemisorption, a useful model has to allow for the electron-electron interaction. To this end Grimley (1967) and Newns (1969) independently introduced the Anderson model (Anderson, 1961), initially worked out for the description of magnetic impurities in alloys. The Anderson model can be solved exactly in the Hartree-Fock (HF) approximation, but also allows for approximate solutions which contain electron correlation effects (Brenig and Schönhammer, 1974).

To define the Anderson-Grimley-Newns (AGN) Hamiltonian for chemisorption, we follow Grimley (1975) and take an orthonormal set $\{\phi_A,\phi_k\}$, where ϕ_A is the adatom orbital and $\{\phi_k\}$ are metal states, which include surface states as well as the conduction states:

$$H=\sum_\sigma E_A n_{A\sigma}+J_A n_{A\uparrow}n_{A\downarrow}+\sum_{k\sigma} E_k n_{k\sigma} + \sum_{k\sigma}(V_{Ak}c^+_{A\sigma}c_{k\sigma}+V_{kA}c^+_{k\sigma}c_{A\sigma}). \tag{2}$$

In Eq. (2) $n_{i\sigma}$ ($i=A,k$) stands for $c^+_{i\sigma}c_{i\sigma}$ and it is the number operator of a spin σ electron in the orbital ϕ_i, with $c^+_{i\sigma}$ and $c_{i\sigma}$ being the creation and annihilation operators in the orbital ϕ_i, respectively. The first two terms of the equation describe noninteracting and interacting electrons in the adatom orbital ϕ_A, the third term describes the noninteracting electrons in the semi-infinite metal in orbitals ϕ_k with energy E_k, while the fourth term (the hopping term) couples the adatom and the metal by allowing them to share all the electrons. The hopping integrals V_{Ak} and V_{kA} determine the charge transfer, and their magnitude is associated with the coupling strength. Since several authors have reviewed the AGN model in detail (Nørskov, 1990; Spanjaard and Desjonquères, 1990), we only outline the main results:

(1) Formally the HF solution is obtained by linearizing the Heinsenberg equations of motion for the operators $\{c_{A\sigma},c_{k\sigma}\}$, i.e., we replace the operator $n_{A\sigma}$ with its expectation value in the HF ground state $\langle n_{A\sigma}\rangle$.

(2) In the original work by Newns, the adsorption energy $E_{\rm ads}$ is expressed as a function of the occupancies $\langle n_{A\uparrow}\rangle$ and $\langle n_{A\downarrow}\rangle$. Detailed consideration shows that the self-consistent solution corresponds to the saddle point of $E_{\rm ads}(\langle n_{A\uparrow}\rangle,\langle n_{A\downarrow}\rangle)$. This method allows for magnetic solutions, i.e., different occupancies with different spins (DODS). In Fig. 1 we show the nonmagnetic and the magnetic behaviors typical of $E_{\rm ads}$ in the framework of Newns' method.

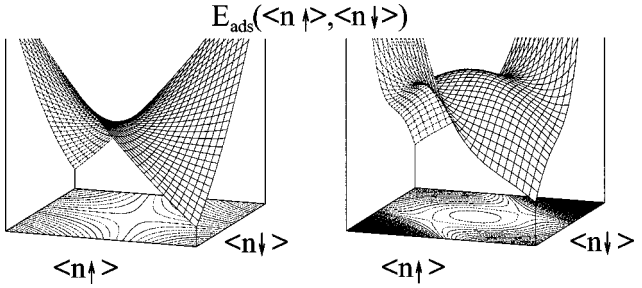

FIG. 1. Nonmagnetic (left) and magnetic (right) solutions (saddle points) of Newns' method for the adsorption energy $E_{\rm ads}$ as a function of occupancies $\langle n_{A\uparrow}\rangle$ and $\langle n_{A\downarrow}\rangle$.

(3) Recall that the relevant parameters of the method are the metal bandwidth W, the hopping strength V, and the Coulomb repulsion on the adatom J_A. The self-consistent solutions for the adatom energy level may lie either outside or inside the metal band. There are different results depending on the relationship between V and W. The solution to be found for $V\gtrsim W$ and a Coulomb repulsion (J_A) as strong as that in the $1s$ level of the H atom shows typical molecular behavior: the electron levels on the adatom and on the metal are split into two "molecular orbitals," a bonding and an antibonding state, one below and one above the metal band, respectively, with a weak continuous part extending over the band. In such a case (the strong-coupling case), the solid is viewed as a big atom coupled with the adatom. In the opposite limit (the weak-coupling case), i.e., for $V\ll W$ and the same J_A as previously, the density of states of the system projected onto the adatom orbital is small except around a narrow range of energies where it is simply broadened to give a Lorentzian-like resonance. This resonant state within the metal band is normally called a "virtual state" (Grimley, 1975). For larger W this resonant state is smeared out.

(4) A clear signature of the many-body character of the HF solution of the AGN model is the calculation of the binding energy $E_{\rm ads}$ of the adatom, which cannot be written as a difference between the sum of the perturbed and unperturbed eigenvalues of the system, but has to include the expectation value of the electron-electron interaction on the adatom:

$$E_{\rm ads}=\left[\sum_{m\sigma}\varepsilon_m^{(\sigma)}-J_A\langle n_{A\uparrow}\rangle\langle n_{A\downarrow}\rangle\right]-\left[2\sum_k E_k+E_A\right], \tag{3}$$

where $\varepsilon_m^{(\sigma)}$ are the Fock eigenvalues.

(5) The results obtained by Newns for the charge transfer on the adatom for H adsorption on some transition metals and the relevant parameters used in the calculations are summarized in Table I, where an elliptical band shape $\Gamma(\epsilon)=\Gamma_0[1-(2\epsilon/W)^2]^{1/2}$ is assumed, and the band height Γ_0 is related to the hopping strength by $2V^2=\Gamma_0/P$ (P is the number of nearest neighbors).

TABLE I. Parameters used and charge transfer to H calculated by Newns. Columns 2 to 4 contain the bandwidth W, the experimental adsorption energies $-E_{\mathrm{ads}}^{\mathrm{exp}}$ [see Newns (1969)] and the band height Γ_0.

Metal	W/Ry	$-E_{\mathrm{ads}}^{\mathrm{exp}}$/Ry	Γ_0/Ry	Charge transfer/ electrons
Ti	0.632	0.228	0.150	0.39
Cr	0.448	0.237	0.152	0.23
Ni	0.279	0.212	0.152	0.16

From such results one can see that, by including the Coulomb repulsions of electrons in the $1s$ orbital, one prevents the formation of H^- adanions.

Approximate solutions beyond the HF approximation (in other words in the large-J_A limit) have been obtained by Brenig and Schönhammer (1974). Such results, which include some correlation effects between the electrons on the adatom, show a smaller charge transfer to the adatom than do the results of Newns.

Though a useful tool in some important respects [for which they have been extended to other adsorbed systems (Grimley, 1975; Spanjaard and Desjonquères, 1990)], calculations based only on the AGN model have gradually been abandoned because:

(a) This model only tries to describe the electron-electron interaction on the adatom and its nearest neighbors' valence orbitals at most, which implies that chemisorption is always a very localized phenomenon.

(b) It determines the interaction between the adatom and metal electrons only by the hopping terms, which cannot take into account the correlation effects.

The desirability of a more extended electron-electron interaction region than that on the adatom has motivated research by other methods, using the Green's-function, slab and supercell, or cluster approaches (see Sec. IV). Theoretical research towards a more accurate solution also seeks to replace the parameters of the AGN model, which are an *ad hoc* constraint of the model, and attempt a more general *ab initio* solution of the chemisorption problem, although with certain limitations to be discussed later on.

Common to all localized solutions, the Friedel sum rule (Friedel, 1954) is not satisfied in the AGN model [see Eqs. (67) and (69) with $\mathcal{Z}=1$]. Owing to the more general character of this failure, it will be discussed later on in Sec. V.B.

In conclusion, important difficulties with the AGN model are that it treats chemisorption at the atom-metal equilibrium distance, which is usually between 1 and $3a_0$ (Bohr radius), and that no single-particle theory working within the HF approximation can describe the correlation-energy contribution. This contribution is essential in any description of the classical image potential, and for molecules it is important at larger distances from the metal surfaces.

B. The Zaremba-Kohn approach to physisorption

In physisorption the particle-metal distances are usually larger and a different treatment of the particle-surface interaction than that provided by the AGN model is required. Since *ab initio* investigations of physisorption on metals are often limited to noble gases, in particular to the lighter ones, which are excellent probes of the surface microscopic profile, theoretical studies of the adiabatic atom-metal interaction concentrate on the ground-state adiabatic potential-energy surface, in the whole interaction region. By exploiting the translational invariance over a periodically ordered surface, one can expand the total atom-metal potential-energy surface $V(\mathbf{R})$ in a Fourier series in terms of the reciprocal 2D lattice vectors $\mathbf{G}$:

$$V(\mathbf{R})=V_0(Z)+\sum_{\mathbf{G}\neq\mathbf{0}} V_{\mathbf{G}}(Z)e^{i\mathbf{G}\cdot\mathbf{R}_\parallel}. \tag{4}$$

The coordinates of the atom are $\mathbf{R}\equiv(\mathbf{R}_\parallel,Z)$, where $\mathbf{R}_\parallel \equiv(\mathbf{X},\mathbf{Y})$ is parallel to the surface and Z orthogonal to it. $V_0(Z)$ is the so-called laterally averaged interaction potential (Bortolani and Levi, 1986), while the components $V_{\mathbf{G}}(Z)$ decrease exponentially and depend on the surface profile or surface corrugation. The corrugation $Z=\zeta(\mathbf{R}_\parallel)$ is a periodic function of the lateral variables, corresponding to the surface of the classical turning points at a fixed atom energy (Rieder, Garcia, and Celli, 1981; Bortolani and Levi, 1986). We shall focus our attention only on $V_0(Z)$, which no unified theory has been able to attain to date for any atom-surface distance.

In this section we shall review two fundamental papers by Zaremba and Kohn (1976, 1977) in which an *ab initio* treatment of $V_0(Z)$ was attempted. The reader is directed to Bruch, Cole, and Zaremba (1997) for a more extensive historical review on physisorption. In the former paper, Zaremba and Kohn showed, in an expansion in terms of the atom-metal interaction, that the first-order contribution to the asymptotic behavior of $V_0(Z)$ (large Z) is zero, while the second-order term, which is a correlation-energy term, displays a polynomial dependence as a function of $1/Z$. This second-order interaction energy, $E^{(2)}$, which is the main result obtained by Zaremba and Kohn for large Z, represents the van der Waals atom-metal potential. Such a potential is expressed in terms of the polarization energy from the interaction of the instantaneous dipole on the atom with the induced charge fluctuations in the solid. The fluctuations are spread on the surface for a distance Z sufficiently large that there is no appreciable overlap between the electronic wave functions of the atom and of the metal. Here the electron density–density response function (Fetter and Walecka, 1971) plays a crucial role. One can write

$$E^{(2)}=-\int d\mathbf{r}\int d\mathbf{r}'\int d\mathbf{x}\int d\mathbf{x}'\frac{1}{|\mathbf{R}+\mathbf{x}-\mathbf{r}|}\frac{1}{|\mathbf{R}+\mathbf{x}'-\mathbf{r}'|}\times\int_0^\infty\frac{d\omega}{2\pi}\chi_a(\mathbf{x},\mathbf{x}',i\omega)\chi_s(\mathbf{r},\mathbf{r}',i\omega), \tag{5}$$

where $\chi_{a,s}$ are the retarded response functions of the adatom and of the surface, respectively. Atomic units, with $e=\hbar=m_e=1$, are used in the equations hereafter.

For large Z an expansion in terms of $1/Z$ leads to the Lifshitz potential (Lifshitz, 1955), which is negative, of the form

$$V_{\mathrm{corr}}(Z)=-\frac{C}{Z^3}-\frac{3CZ_0}{Z^4}+O(Z^{-5})$$

$$=-\frac{C}{(Z-Z_0)^3}+O(Z^{-5}). \tag{6}$$

The coefficient C can be expressed in terms of the dielectric function $\epsilon(\omega)$ of the bulk, determined, for example, by optical data, and the dipole polarizability of the atom $\alpha(\omega)$:

$$C=\frac{1}{4\pi}\int_0^\infty d\omega\,\alpha(i\omega)\frac{\epsilon(i\omega)-1}{\epsilon(i\omega)+1}, \tag{7}$$

while Z_0, the position of the reference plane with respect to which the Lifshitz potential is defined, is computed as an appropriate weighted average of the centroid $\bar{z}(i\omega)$ of the induced surface charge:

$$Z_0=\frac{1}{2\pi C}\int_0^\infty d\omega\,\alpha(i\omega)\frac{\epsilon(i\omega)-1}{\epsilon(i\omega)+1}\bar{z}(i\omega). \tag{8}$$

A detailed derivation of Eqs. (6), (7), and (8) can be found in Bruch, Cole, and Zaremba (1997). As an application, Zaremba and Kohn concentrate mainly on a Xe atom on noble metals, showing that the polarization energy, calculated as above, gives the main contribution to the binding energy of the atom (Cohen, Unguris, and Webb, 1975).

In the second paper, Zaremba and Kohn (1977) also treat the interaction, which is repulsive, between a helium atom and a metal at shorter distances, where some overlap between the atomic and the metallic wave functions exists. In calculating such a potential, it is important to consider explicitly the electronic exchange between the atom and the metal. Zaremba and Kohn considered a HF treatment by an expansion, whose characteristic parameter is the overlap (exponentially decaying with Z) between the densities of the unperturbed metal and the atom. In practice, the repulsive energy at first order in such an expansion is due to the change in the single-particle density of states which results from the noble atom–metal overlap. The semiinfinite metal is described by an electron gas interacting with a positive uniform background of density equal to the spatial average of the ion charge distribution (jellium). The only parameter of jellium is the radius r_s of an effective sphere containing one valence electron, which is expressed in units of a_0.

To summarize, the two Zaremba and Kohn papers separate the total physisorption atom-metal potential $V_0(Z)$ into two parts: a short-range HF part $V_{\mathrm{HF}}(Z)$ and a long-range van der Waals contribution, say $V_{\mathrm{corr}}(Z)$, already described:

$$V_0(Z)=V_{\mathrm{HF}}(Z)+V_{\mathrm{corr}}(Z). \tag{9}$$

In Fig. 2 we show Zaremba and Kohn's results for the physisorption potential for He on the noble metals modeled by jellium, as calculated by Eq. (9). Observe that the potentials $V_{\mathrm{corr}}(Z)$ for He on Cu and He on Ag are very similar, while that of He on Au differs significantly depending on the metal work function. Since for noble gas–metal physisorption systems the reference plane position is less than $0.5a_0$ outside the jellium edge, we are far from the point Z_0 where the van der Waals potential and hence $V_0(Z)$ is singular. To avoid such divergence, interpolation schemes have been devised (Tang and Toennies, 1984; Persson and Harris, 1987).

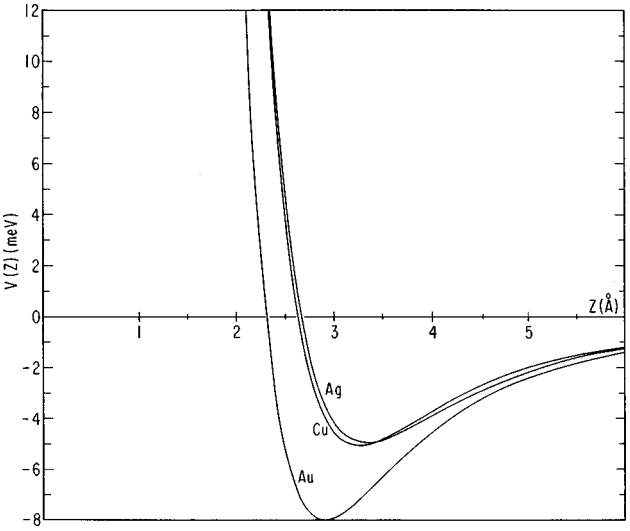

FIG. 2. Physisorption potentials for He on noble metals from the jellium edge. From Zaremba and Kohn (1977).

In conclusion, the longer-range physisorption potential between a particle and a metal allows one to address critical issues not only concerning the importance of exchange and correlation for these phenomena, but also concerning any one-electron treatment in adsorption theory, even if self-consistent.

III. DENSITY-FUNCTIONAL THEORY

A. Generalities

In adsorption theory, as in solid-state and chemical physics, the density-functional approach has become more and more widely used. Most *ab initio* results are now worked out in this framework. The main advantage of the density-functional method, compared to other *ab initio* approaches based on the HF method, such as the configuration-interaction method (Szabo and Ostlund, 1982), is that it solves a one-electron self-consistent equation by using a local potential. This potential allows one to take into account exchange and correlation effects. The density-functional method is also superseding the configuration-interaction method for large molecules because the configuration interaction scales so unfavorably with molecular size (Pacchioni, 1995).

Density-functional theory has been the subject of thorough articles (Jones and Gunnarsson, 1989; Becke, 1995; Kohn, Becke, and Parr, 1996) and books (Parr and

Yang, 1989; Dreizler and Gross, 1990). Therefore we shall only recall a few salient features of this approach. First, in density-functional theory the fundamental variable for a system of N interacting electrons is the electronic charge density $\rho(\mathbf{r})$, following two well-known theorems by Hohenberg and Kohn (1964). Second, in order to obtain the adiabatic electronic properties of the ground state, one works with an effective single-particle Schrödinger equation, the Kohn-Sham equation (Kohn and Sham, 1965). In such an equation one introduces an effective one-electron potential $v_{\text{eff}}(\mathbf{r})$ which provides the same electron density of the ground state, $\rho_0(\mathbf{r})$, as that of the interacting electron system. The Kohn-Sham equation can be written

$$-\frac{1}{2}\nabla^2\psi_i(\mathbf{r})+v_{\text{eff}}(\mathbf{r})\psi_i(\mathbf{r})=\varepsilon_i\psi_i(\mathbf{r}), \tag{10}$$

where

$$v_{\text{eff}}(\mathbf{r})=v(\mathbf{r})+V_{\text{H}}(\mathbf{r})+\frac{\delta}{\delta\rho(\mathbf{r})}E_{xc}[\rho]. \tag{11}$$

In Eq. (11) $v(\mathbf{r})$ is an external potential that may be the ionic one, $V_{\text{H}}(\mathbf{r})$ is the classical Hartree potential, and E_{xc} is the exchange-correlation energy functional, whose functional derivative with respect to $\rho(\mathbf{r})$ gives the exchange-correlation potential $V_{xc}(\mathbf{r})$. The electron density $\rho(\mathbf{r})$ is given by the sum of the squared moduli of the N lowest occupied eigenstates $\psi_i(\mathbf{r})$ with eigenvalues ε_i:

$$\rho(\mathbf{r})=\sum_{i=1}^{N}|\psi_i(\mathbf{r})|^2. \tag{12}$$

The Kohn-Sham equation has to be solved self-consistently because the potential $v_{\text{eff}}(\mathbf{r})$ depends on the charge density. Other methods of solving the Kohn-Sham equation have been proposed. In particular, the Car-Parrinello method allows for a simultaneous optimization of the electron wave function and the ionic coordinates (Car and Parrinello, 1985; Galli and Parrinello, 1991). Steepest-descent (Press *et al.*, 1989) or first-order dynamics and the conjugate-gradient techniques (Stich *et al.*, 1989; Payne *et al.*, 1992) are also commonly used.

After completing the minimization procedure, one can write down the ground-state total energy as a functional of $\rho_0(\mathbf{r})$ as

$$E[\rho_0]=\sum_{i=1}^{N}\varepsilon_i-\frac{1}{2}\int d\mathbf{r}\,V_{\text{H}}(\mathbf{r})\rho_0(\mathbf{r}) -\int d\mathbf{r}\,V_{xc}(\mathbf{r})\rho_0(\mathbf{r})+E_{xc}[\rho_0]. \tag{13}$$

Finally we observe that in the Kohn-Sham approach all the complexity of the many-body problem in density-functional theory is now contained in the exchange-correlation functional.

B. The local-density approximation

A first attempt at obtaining the exchange-correlation energy functional is the local-density approximation (LDA):

$$E_{xc}[\rho]\sim E_{xc}^{\text{LDA}}[\rho(\mathbf{r})]=\int d\mathbf{r}\,\rho(\mathbf{r})\varepsilon_{xc}(\rho(\mathbf{r})), \tag{14}$$

where $\varepsilon_{xc}(\rho(\mathbf{r}))$ is the exchange-correlation energy per particle in a homogeneous electron gas, whose density ρ_{hom} is defined to be that appropriate to the position $\mathbf{r}$, i.e., $\rho_{\text{hom}}=\rho(\mathbf{r})$. The corresponding LDA exchange-correlation potential is

$$V_{xc}^{\text{LDA}}(\mathbf{r})=\frac{\partial}{\partial\rho}\rho\varepsilon_{xc}(\rho)\big|_{\rho=\rho(\mathbf{r})}. \tag{15}$$

$\varepsilon_{xc}(\rho(\mathbf{r}))$ can be obtained using an interpolation procedure between analytic asymptotic behaviors (Hedin and Lundqvist, 1971; Gunnarsson and Lundqvist, 1976; Vosko, Wilk, and Nusair, 1980; Perdew and Zunger, 1981) or one based on a Monte Carlo calculation (Ceperley, 1978; Ceperley and Alder, 1980).

C. Beyond the LDA

1. Spin extension

A widely used improvement to the LDA consists in generalizing the total energy in Eq. (13) to be a functional of the spin density $\rho^{\alpha}(\mathbf{r})$ where the index α ($\uparrow$ or $\downarrow$) denotes spin up or down. Von Barth and Hedin (1972) presented first a formal justification of the spin-density-functional theory, which replaces the ground-state energy functional in Eq. (13) for a spin-independent potential $v(\mathbf{r})$, with

$$E[\rho_0]=\sum_{i=1}^{N}\sum_{\sigma}\varepsilon_i^{(\sigma)}-\frac{1}{2}\int d\mathbf{r}\,V_{\text{H}}(\mathbf{r})\rho_0(\mathbf{r}) -\sum_{\sigma}\int d\mathbf{r}\,V_{xc}^{(\sigma)}([\rho_0^{\uparrow},\rho_0^{\downarrow}];\mathbf{r})\rho_0^{\sigma}(\mathbf{r})+E_{xc}[\rho_0^{\uparrow},\rho_0^{\downarrow}], \tag{16}$$

where $\rho_0(\mathbf{r})=\rho_0^{\uparrow}(\mathbf{r})+\rho_0^{\downarrow}(\mathbf{r})$. One then obtains the correct ground-state charge density $[\rho_0^{\uparrow}(\mathbf{r}),\rho_0^{\downarrow}(\mathbf{r})]$ after solving (self-consistently) the following pair of coupled Kohn-Sham equations:

$$-\frac{1}{2}\nabla^2\psi_{i\alpha}(\mathbf{r})+[v(\mathbf{r})+V_{\text{H}}(\mathbf{r})+V_{xc}^{(\alpha)}([\rho^{\uparrow},\rho^{\downarrow}];\mathbf{r})]\psi_{i\alpha}(\mathbf{r}) =\varepsilon_i^{(\alpha)}\psi_{i\alpha}(\mathbf{r}). \tag{17}$$

As pointed out by Jones and Gunnarsson (1989), the exact density-functional theory shows that it is possible to determine the total energy using a functional dependent on the charge density alone. Hence no spin dependence need be considered. In practice, however, it is necessary to find a working approximation to the exchange and correlation functionals, $E_{xc}^{\text{approx}}[\rho]$. This task is performed by introducing the local-spin-density approximation (LSDA). Many LSDA have been proposed for the correlation-energy functional (van Barth and Hedin, 1972; Gunnarsson and Lundqvist, 1976; Vosko, Wilk, and Nusair, 1980; Perdew and Zunger, 1981). Such functionals provide the simplest way to fulfill Hund's rule and a satisfactory description of a system with un-

paired electrons, giving, for example, the cohesive energy of the alkali metals closer to the experimental values (Gunnarsson, Lundqvist, and Wilkins, 1974). A density-functional–LSDA calculation of magnetism of $3d$, $4d$, and $5d$ transition metal single adatoms on Cu(001) and Ag(001), and on Pd(001) and Pt(001) have been recently presented by Lang *et al.* (1994) and Stepanyuk *et al.* (1996). A comparison of these results with those obtained on a jellium surface by the same density-functional–LSDA method will be discussed in a forthcoming publication (Trioni, Palumbo, and Brivio, 1998).

2. Self-interaction correction

In the many-electron problem one has to take into account that the electrostatic potential felt by an electron is due to all the other electrons but itself. In other words, one has to subtract the so-called self-interaction correction from the electron-electron potential. In the HF approach there is an exact cancellation of the self-interaction contribution between the Hartree and the exchange potentials. In the LSDA, this simplification is not included, and an explicit correction has to be considered. We follow the Perdew and Zunger (1981) approach to this problem. To subtract the self-interaction correction from the total energy of the many-electron system one can write the following exchange-correlation functional:

$$E_{xc}^{\mathrm{SIC}}[\rho]=E_{xc}^{\mathrm{approx}}[\rho]-\sum_{i\sigma}\ \delta_{i\sigma}. \tag{18}$$

The summation is over all occupied orbitals, and

$$\delta_{i\alpha}=\frac{1}{2}\int d\mathbf{r}\int d\mathbf{r}'\frac{\rho_i^{\alpha}(\mathbf{r})\rho_i^{\alpha}(\mathbf{r}')}{|\mathbf{r}-\mathbf{r}'|}+E_{xc}^{\mathrm{approx}}[\rho_i^{\alpha},0]. \tag{19}$$

In Eq. (19), the first term represents the exact Coulomb self-interaction energy, while the second is the self-exchange/correlation energy of a single fully occupied orbital calculated by the same approximation. This correction is exact for a one-electron system (see the H atom). The approximation involved in $E_{xc}^{\mathrm{approx}}[\rho]$ can be the LSDA, the gradient expansion (see next section), or any other. Note that the functional in Eqs. (18) and (19) gives an effective potential which depends on the Kohn-Sham eigenstates and is therefore orbital dependent.

Other self-interaction corrections, very similar to that in Eqs. (18) and (19), have been proposed (Stoll, Pavlidov, and Preuss, 1978; Vosko and Wilk, 1983; Cortona, 1986). The self-interaction correction is most important in atomic calculations, where the electron density is quite inhomogeneous. In adsorption problems it has only been used within the framework of phenomenological models which are not discussed in this review (Cortona *et al.*, 1992; Cvetko *et al.*, 1994).

3. Gradient correction

The first attempt to include a certain nonlocality in the exchange-correlation functional via the density gradient is found in the original paper of Hohenberg and Kohn (1964). Subsequently, Kohn and Sham (1965) proposed a first-order correction to the LSDA for a slowly varying density ρ^{α}. In this case the exchange-correlation energy functional E_{xc}^{GEA} can be written as

$$E_{xc}^{\mathrm{GEA}}[\rho^{\uparrow},\rho^{\downarrow}]=E_{xc}^{\mathrm{LSD}}[\rho^{\uparrow},\rho^{\downarrow}]+\sum_{\sigma,\sigma'}\int d\mathbf{r}\ \ C(\rho^{\sigma},\rho^{\sigma'})\frac{\nabla\rho^{\sigma}\cdot\nabla\rho^{\sigma'}}{(\rho^{\sigma}\rho^{\sigma'})^{2/3}}, \tag{20}$$

where $C(\rho^{\sigma},\rho^{\sigma'})$ is a weakly varying function of ρ^{σ} and $\rho^{\sigma'}$ (Rasolt and Geldart, 1986). This gradient expansion approximation has produced better results only when the electron density of the investigated system is indeed slowly varying (Kohn and Vashishta, 1983), which is not the case for atoms and molecules.

On the other hand, a generalized gradient approximation for the exchange-correlation energy functional E_{xc}^{GGA} of the form

$$E_{xc}^{\mathrm{GGA}}[\rho^{\uparrow},\rho^{\downarrow}]=\int d\mathbf{r}\ \ f(\rho^{\uparrow},\rho^{\downarrow},\nabla\rho^{\uparrow},\nabla\rho^{\downarrow}) \tag{21}$$

may produce much more accurate results than the LDA. Note that Eq. (20) is a truncated series in a $\nabla\rho$ expansion of the true but unknown exchange-correlation functional. But the function $f(\rho^{\uparrow},\rho^{\downarrow},\nabla\rho^{\uparrow},\nabla\rho^{\downarrow})$ in Eq. (21) can be cast in such a way as to effectively sum up an infinite series in powers of $\nabla\rho$.

We shall now try to explain why the gradient expansion approximation gives worse results than the LDA, while the generalized gradient approximation gives much better ones for most systems. We introduce the so-called exchange-correlation hole $\rho_{xc}(\mathbf{r},\mathbf{r}')$. Recall the first-order density matrix (March, 1983)

$$\rho_1(\mathbf{x},\mathbf{x}')=N\int d\mathbf{x}_2\int d\mathbf{x}_3\ldots\int d\mathbf{x}_N\Psi^*(\mathbf{x},\mathbf{x}_2,\mathbf{x}_2,\ldots,\mathbf{x}_N)\times\Psi(\mathbf{x}',\mathbf{x}_2,\mathbf{x}_2,\ldots,\mathbf{x}_N), \tag{22}$$

with $\mathbf{x}=(\mathbf{r},\sigma)$. Hence the electron density is given by

$$\rho(\mathbf{r})=\sum_{\sigma}\ \rho^{\sigma}(\mathbf{r})=\sum_{\sigma}\ \rho_1(\mathbf{r},\sigma,\mathbf{r},\sigma). \tag{23}$$

We also need the pair-correlation function (or the diagonal part of the second-order density matrix):

$$\rho_2(\mathbf{x},\mathbf{x}')=\frac{N(N-1)}{2}\int d\mathbf{x}_3\ldots\int d\mathbf{x}_N\Psi^*(\mathbf{x},\mathbf{x}',\mathbf{x}_3,\ldots,\mathbf{x}_N)\times\Psi(\mathbf{x},\mathbf{x}',\mathbf{x}_3,\ldots,\mathbf{x}_N). \tag{24}$$

Then the exchange-correlation hole can be defined by

$$\rho_{xc}(\mathbf{r},\mathbf{r}')=\frac{2\rho_2(\mathbf{r},\mathbf{r}')-\rho(\mathbf{r})\rho(\mathbf{r}')}{\rho(\mathbf{r})}, \tag{25}$$

where

$$\rho_2(\mathbf{r},\mathbf{r}')=\sum_{\sigma\sigma'}\ \rho_2(\mathbf{r},\sigma,\mathbf{r}',\sigma'). \tag{26}$$

In Eq. (25) the factor 2 comes from double counting in the electron-electron repulsion term. In practice, the expression in Eq. (25) simply defines ρ_{xc} as the total pair-correlation function minus the classical Hartree term. In particular, the exchange part $\rho_x^\alpha(\mathbf{r},\mathbf{r}')$ can be written as

$$\rho_x^\alpha(\mathbf{r},\mathbf{r}') = -\frac{|\rho_1(\mathbf{r},\alpha,\mathbf{r}',\alpha)|^2}{\rho^\alpha(\mathbf{r})}. \tag{27}$$

Note that in a representation on a basis set $\{\psi_{i\alpha}(\mathbf{r})\}$, Eq. (27) becomes

$$\rho_x^\alpha(\mathbf{r},\mathbf{r}') = \frac{1}{\rho^\alpha(\mathbf{r})} \sum_{i,j\in \mathrm{occ}} \psi_{i\alpha}^*(\mathbf{r})\psi_{j\alpha}^*(\mathbf{r}')\psi_{j\alpha}(\mathbf{r})\psi_{i\alpha}(\mathbf{r}'). \tag{28}$$

Consequently the correlation hole $\rho_c(\mathbf{r},\mathbf{r}')$ is

$$\rho_c(\mathbf{r},\mathbf{r}') = \rho_{xc}(\mathbf{r},\mathbf{r}') - \sum_\sigma \frac{\rho^\sigma(\mathbf{r})\rho_x^\sigma(\mathbf{r},\mathbf{r}')}{\rho(\mathbf{r})}. \tag{29}$$

Apart from providing a compact way to write down the corresponding energy functional, the exchange and the correlation holes obey the following well-known exact properties (Gunnarsson and Lundqvist, 1976; Perdew, 1985):

$$\rho_x(\mathbf{r},\mathbf{r}') \leqslant 0, \tag{30}$$

$$\int d\mathbf{r}'\,\rho_x(\mathbf{r},\mathbf{r}') = -1 \quad \text{for any } \mathbf{r}, \tag{31}$$

$$\int d\mathbf{r}'\,\rho_c(\mathbf{r},\mathbf{r}') = 0 \quad \text{for any } \mathbf{r}. \tag{32}$$

Equations (30) and (31) tell us that the exchange hole density is strictly negative and that the exchange hole contains exactly one electron. In practice, the exchange hole reduces the Coulomb repulsion since, due to the Pauli principle, parallel-spin electrons tend to avoid each other. The conditions in Eqs. (30), (31), and (32) are satisfied by the LSDA, since the LSDA exchange-correlation hole is that of a physical system, i.e., the homogeneous electron gas. This explains why the LSDA gives realistic values for the electronic properties of several systems that are not homogeneous. In contrast, the exchange-correlation hole of the gradient expansion does not belong to any possible physical system, as it originates from a truncated expansion of the LSDA, and hence it violates all the above conditions.

These observations led to a new class of correction, the generalized gradient approximation (GGA), fulfilling the constraints in Eqs. (30), (31), and (32). For a review see Perdew (1995). This approximation achieved much better accuracy in the calculated electronic properties than that obtained by the LSDA, for a wide range of systems. Many GGA corrections are now available. They are built up by fitting various sets of *ab initio* results together with the known asymptotic behaviors. A widely used nonlocal approximation of the exchange-correlation energy functional was introduced by Becke (1988) for the exchange part, and by Lee, Yang, and Parr (1988) for the correlation part. In combination, their approach is sometimes known as the B-LYP generalized gradient approximation. As an example, consider the exchange energy E_x^{GGA}, which comes from an extension of the LDA,

$$E_x^{\mathrm{LDA}} = -\frac{3}{2}\left(\frac{3}{4\pi}\right)^{1/3} \sum_\sigma \int d\mathbf{r}(\rho^\sigma)^{4/3}. \tag{33}$$

The corresponding Becke-Lee-Yang-Parr GGA is given by

$$E_x^{\mathrm{GGA}} = E_x^{\mathrm{LDA}} - \beta \sum_\sigma \int d\mathbf{r}(\rho^\sigma)^{4/3} \frac{(x^\sigma)^2}{1+6\beta x^\sigma \sinh^{-1} x^\sigma}, \tag{34}$$

with $x^\alpha = |\nabla\rho^\alpha|/(\rho^\alpha)^{4/3}$, and $\beta = 0.0042$ a.u. to give the best fit of atomic Hartree-Fock data. The correlation functional can be found in Lee, Yang, and Parr (1988).

Following the same spirit and by using a very similar exchange functional to that of Becke in Eq. (34), Perdew *et al.* (1992) suggested a more general GGA functional satisfying a greater number of criteria for the homogeneous gas limit than Eqs. (30), (31), and (32), and without any fitting parameters. In practice, in order to build up a correct GGA, Perdew *et al.* (1992) start with the gradient expansion approximation and then cut off spurious long-range parts to restore the exact properties of Eqs. (30), (31), and (32) and some scaling conditions (Levy and Perdew, 1985).

The improvement in the results is significant in many fields of atomic and molecular physics. Perdew (1995) reports results (the errors are in parentheses) for exchange and correlation energies of He (1% and 10%) and Ne (0.05% and 2%), atomization energies of C_2 (3%) and C_6H_6 (3%), and lattice constants of Li (1%) and Na (0.1%). Comparison of results obtained with different GGA's is available in the literature, all confirming the great improvement obtained by such an approximation (Johnson, Gill, and Pople, 1993; Filippi, Gonze, and Umrigar, 1996; Seminario, 1996).

Nevertheless, any of the above GGA's fail in describing the interaction between an electron and its hole when they stay far apart. Only an exchange-correlation potential not based on the LDA could describe the van der Waals interaction or the image potential felt by an electron outside a metal surface.

In conclusion, the GGA represents an extremely useful tool for obtaining better adiabatic electronic properties than the LDA for several inhomogeneous systems. However, while the LDA is expected to be a milestone in the *ab initio* studies of many-electron systems, it remains questionable whether the generalized gradient approximation shares the same fundamental importance or is only a very practical step in the search of the correct nonlocal exchange-correlation functionals.

IV. ADSORPTION MODELS

A. The cluster approach

Originally the idea of a cluster of metal atoms, representing an extended substrate plus the adsorbate, was

related to the study of catalysts. One also expected to avail oneself of the concepts and computational methods developed in theoretical chemistry by assuming that chemisorption is essentially a localized phenomenon. But often the correct number of substrate atoms to include in a realistic calculation is difficult to determine (Messmer, 1979). The related problem of the finite size of the cluster system (which may generate a significant number of undercoordinated atoms) is resolved in different ways according to whether the dangling bonds of the cluster are mainly covalent, ionic, or metallic. In the first case such dangling bonds are saturated, often with hydrogen atoms (Sauer, 1989), while for the ionic case an external electric field is added to the system to simulate the Madelung field at the border of the cluster (Colbourn, 1992). A fixed external dipole potential is sometimes used as an approximation to the electric field which exists on the surface region of the metals (Hermann, 1992).

For chemisorption on metals perhaps the most important question regards the convergence of the adsorption energy, which oscillates with cluster size and shape. As discussed in te Velde and Baerends (1993) small changes in the cluster size may, for example, shift the main cluster acceptor orbital from below to above the Fermi energy, and hence drastically change the interaction with the adsorbate. There are treatments which try to avoid this problem (Panas *et al.*, 1988; see also Siegbahn, Nygren, and Wahlgren, 1992; Zonnevylle, Geerlings, and van Santen, 1994). Other methods, such as the slab and the supercell approaches, which retain 2D or 3D periodic boundary conditions for the wave functions, or the embedding approach, which takes into account a semi-infinite solid, seem to be more suitable for treating adsorption on metals.

However, the cluster approach is still very popular among theoretical chemists, owing in part to the computational resources now available, which allow one to treat several cluster atoms. This approach has been amply reviewed recently (Pacchioni, 1995; Whitten and Yang, 1996).

B. The embedded adsorbate

The embedding method attempts to provide an accurate description of the interacting electrons of the system constituted by the molecule and that part of the substrate close to it, while the electronic properties of the rest of the metal are assumed to be unperturbed by the adsorbate. One would also like to be able to consider a continuous electronic spectrum due to the semi-infinite nature of the substrate, since the adsorbate may form resonant states to be displayed as peaks with some width in the local density of states. When the electronic properties of the molecule plus a cluster region around it (embedding region) are computed by considering the properties of the surrounding semi-infinite solid, this approach is often called the *embedding approach* (see Fig. 3).

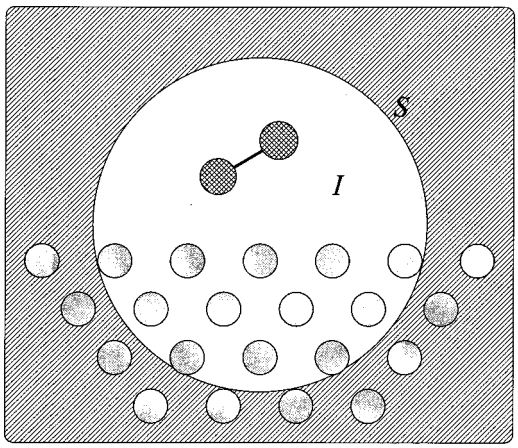

FIG. 3. Simple picture of the embedding of a diatomic molecule into a semi-infinite solid, whose embedding region surface is denoted by S. Note that the embedding region I is a sphere just for the sake of simplicity.

The first attempt by the Green's-function method to perform an embedded cluster calculation of an adatom on a simple metal, described by cubium, was proposed by Grimley and Pisani (1974). Owing to limited computer facilities, they were able only to project the substrate properties onto the nearest neighbor atom to the adatom.

Common to the Grimley and Pisani's (1974) pioneering work and to most of the embedding approaches that calculate the electronic properties of chemisorbed species on metals is the Green's-function formalism, which describes well the continuous distribution of the substrate states (Grimley, 1976). Furthermore, the Green's-function method allows for a natural connection between the electronic properties of the embedding region and the substrate regions either in terms of a Dyson's equation (Gunnarsson and Hjelmberg, 1975; Pisani, 1978; Williams, Feibelman, and Lang, 1982; Scheffler *et al.*, 1991) or by matching techniques (Inglesfield and Benesh, 1988a; Trioni *et al.*, 1996). In all methods the single-particle approximation for the electrons of the system is essential in the problem.

1. Methods based on the Dyson equation

We review first the embedding methods based on the Dyson equation.

The Green's operator for the full system adsorbate plus semi-infinite substrate is given by the well-known expression

$$G(z)=(zI-H)^{-1}, \tag{35}$$

where I is the identity operator, H the Hamiltonian of the system, and z a complex energy. Depending on the first-principles method used in the calculation, HF or density-functional theory, the one-electron effective Hamiltonian H could be based on the Fock model, or the Kohn-Sham model of Eq. (10).

Of course the solution of Eq. (35) implies an expansion of $G(z)$ on a complete basis set of orbitals, say

$\{\psi_i\}$. The choice of such a basis set is often related to the character (mainly localized or not) of the metal orbitals, but often stems from the personal background of the involved scientist (either a theoretical chemist or a solid-state physicist).

Assume now that the matrix elements of all operators, expanded on a suitable basis set, say in the $\{\psi_i\}$ representation, are considered. Indicate the unperturbed Hamiltonian (to be defined in the following) with H_0 and its Green's function G_0. Formally the solution of Eq. (35) is given by the Dyson (or Lippmann-Schwinger) equation:

$$G = G_0 + G_0 M G, \tag{36}$$

which can always be written as

$$G = (I - G_0 M)^{-1} G_0. \tag{37}$$

Here M is the perturbing potential, which is generally a complex self-energy, defined by

$$M = (zS - H_0) - G^{-1}(z), \tag{38}$$

where the term S represents the overlap matrix. Of course the definition of M depends on the choice of H_0. In the embedding theory framework, observe that the Dyson equation (36) can be viewed as a powerful way of recasting the Schrödinger equation for the electron stationary states elastically scattering off the potential M (Taylor, 1972).

It is interesting to note that the choice of unperturbed (reference system) Hamiltonian H_0 within the embedding region is fairly arbitrary. See, for example, Gunnarsson and Hjelmberg (1975), Grimley (1976, 1983), and Scheffler *et al.* (1991). We require only that it represents the clean surface and the semi-infinite metal outside the embedding region.

Then to make progress in the calculation of G, approximations are required. Note that an obvious limitation for all methods is the finiteness of the basis set on which the operators are expanded. In the approaches by Pisani (1978), Williams, Feibelman, and Lang (1982), Scheffler *et al.* (1991), and Wachutka *et al.* (1992), such a basis set is constituted by localized orbitals defined within the embedding region. The other approximation common to all methods is the finite size of the embedding region, where one solves self-consistently the Dyson equation. If the size of the embedding region tends to infinity, the solution obtained by all embedding methods approaches the exact one. Of course the above statement holds if there is no restriction in the basis set and in the electron-electron interaction description.

The new idea of the method proposed by Williams, Feibelman, and Lang (1982) is to expand all operators on a finite basis set, which is different in the perturbed and unperturbed case. Since by this method, still based on the density-functional theory, several interesting results have been obtained (see Sec. VII), we consider it worthwhile to discuss in some detail the Dyson equation used in this work:

$$G(z) = G_0(z) + G_0(z)(\delta H - z\,\delta S)G(z). \tag{39}$$

In Eq. (39) δH and δS are the matrix elements of the Hamiltonian and of the overlap term, constructed on suitable basis sets of localized wave functions, which vary in the perturbed and unperturbed cases. $G_0(z)$ is the matrix element of the adsorbate-free substrate Green's function, obtained from a previous calculation (e.g., using a slab geometry). This procedure allows one to optimize the selection of the basis functions and to reduce the size of all matrices to be inverted without any further approximation, differently from the Gunnarson and Hjelmberg (1975) method. In practice, Williams, Feibelman, and Lang (1982) expand each operator on a suitable basis set from the very beginning, and then only carry out matrix calculations. In this method addition of chemisorbed atoms requires additional basis functions, so that the matrices of the perturbed problem are larger than those of the unperturbed problem. This is performed in the calculation by adding some diagonal blocks to the matrices of the unperturbed system.

By making use of the concept of the "ideal" Green's-function matrix (Williams, Feibelman, and Lang, 1982) it is also possible to reduce the dimensions of the matrices enough to permit modeling of surfaces and vacancies including the self-consistent electronic response. In the original work, Williams, Feibelman, and Lang (1982) consider how the previous ideas can be combined to solve the problem of the chemisorption of a molecule on a solid surface. The final Dyson equation describing the molecule-surface interaction for the Green's-function matrix $G(z)$ is

$$G(z) = G_{MS}(z) + G_{MS}(z)(\delta H - z\,\delta S)G(z). \tag{40}$$

In this equation a full hierarchy of Dyson equations, all to be solved self-consistently, is implied. First these authors consider the formation of a molecule from two atoms, next the formation of the surface by the use of the "ideal" Green's-function matrix from an infinite solid. Finally the chemisorbed molecule is formed from the free molecule and the bare surface, both described by the Green's-function matrix $G_{MS}(z)$. The term $\delta H - z\,\delta S$ accounts for the coupling of the molecule and the substrate as well as the changes in the molecule and in the surface that result from this new coupling.

A self-consistent Green's-function embedding method within the density-functional theory has also been proposed more recently by Scheffler *et al.* (1991) and Wachutka *et al.* (1992). Here the Kohn-Sham Hamiltonian is split into two parts:

$$H = H_0 + \Delta V, \tag{41}$$

where H_0 is the Hamiltonian of a semi-infinite crystal and ΔV the effective potential of the adsorbate system. One obtains an equation for the difference of the exact and the unperturbed Green's operator $\Delta G(z)$ in the following way:

$$\Delta G(z) = G_0(z)\Delta V[I - G_0(z)\Delta V]^{-1} G_0(z). \tag{42}$$

The important quantity is the change in the density of electrons:

$$\Delta\rho(\mathbf{r}) = -\frac{2}{\pi}\mathrm{Im}\int_{-\infty}^{E_F} d\varepsilon\,\Delta G(\mathbf{r},\mathbf{r};\varepsilon). \tag{43}$$

At this stage, as well as in the Gunnarsson and Hjelmberg (1975) approach, Eqs. (42) and (43) are projected onto a basis set $\{\chi_i(\mathbf{r})\}$. After choosing a basis set of sufficient flexibility to represent several meaningful localized functions, one can write $\Delta\rho(\mathbf{r})$ as

$$\Delta\rho(\mathbf{r})=\sum_{i,j}\Delta\rho_{ij}\chi_i(\mathbf{r})\chi_j^*(\mathbf{r}). \tag{44}$$

The functions $\{\chi_i(\mathbf{r})\}$ cover the embedding region. We solve Eq. (42) by using self-consistently the results of Eqs. (43) and (44).

The methods of Williams, Feibelman, and Lang (1982) and Scheffler *et al.* (1991) share the same fundamental physics, but differ on a matter of computational convenience. In this respect, as pointed out by Scheffler *et al.* (1991) and Feibelman (1992b), the main difference between the two approaches is in the treatment of the kinetic energy. In the method of Feibelman (1992b) δH in Eq. (39) contains a kinetic-energy contribution which has a longer range than that suggested by the screening length of the perturbation induced by the adsorbate. On the other hand, in the approach of Scheffler *et al.* (1991) the full kinetic energy is contained in the zeroth-order description, in other words, in the unperturbed Green's function G_0. Consequently the potential ΔV in Eq. (42) has a shorter range, so the solution can be obtained from smaller sets of equations. For this reason, and in order to improve the calculation efficiency of his method, Feibelman (1992b) first notes that the kinetic-energy matrix does not depend on the density of electrons $\rho(\mathbf{r})$ and then modifies his approach by taking the kinetic-energy matrix out of the self-consistent loop.

Still based on some concepts of embedding is the approach of Lang and Williams (1978). These authors introduce a formalism in which the unknowns are the electronic wave functions not the Green's function. The Lippmann-Schwinger equation is used to correctly match the wave functions inside the region, where the adatom perturbation is effective and the density-functional–LDA calculation is performed, to those in the region outside it. This is a semi-infinite metal described by the jellium model. Since one obtains the electronic wave functions by numerical integration, no expansion on a basis set in a localized region is required. The fact that the method is suited to a very particular substrate (jellium) represents the limitation of the Lang and Williams (1978) approach compared to the embedding treatments just outlined.

2. Methods based on Green's-function matching

Although the Green's-function matching method is an approach for determining the Green's function of an adsorbate system embedded in a metal, it is not based upon the Dyson equation (Inglesfield, 1981; Inglesfield and Benesh, 1988a; Trioni *et al.*, 1996). It has been widely applied to calculations of the properties of clean surfaces (Benesh and Liyanage, 1994) and adsorbed overlayers (Ishida, 1990). More recently it has been applied to the single adsorbate problem (Trioni *et al.*, 1996). In this method one sets up an effective Schrödinger equation within a localized region (the embedded region) containing the adsorbate and that region of the substrate which we assume to be mainly perturbed by the adsorbate. The influence of the extended substrate enters in the form of a nonlocal energy-dependent potential to be determined from the Green's function of the substrate in the absence of the adsorbate. Eventually all the relevant physical quantities are obtained as in other methods by projecting the equation onto a suitable basis set. However, unlike methods based upon the Dyson equation, the boundary conditions do not enter following an expansion throughout the embedded volume, giving more flexibility for the choice of the basis set. In addition, this method is based upon a variational solution of the Schrödinger equation, without any *a priori* biasing in the behavior of the Green's function.

A *variational* solution to the single-particle Schrödinger equation may be found which explicitly depends only upon the wave function in the embedding region I, the region of interest. To do this one constructs a trial wave function $\phi(\mathbf{r})$, which is to be varied within region I and which in region II, the rest of the extended system containing the substrate, is a solution $\psi(\mathbf{r})$ of the Schrödinger equation for the unperturbed system at energy ε. On the surface S which divides the two volumes I and II, the trial wave function is continuous, $\phi(\mathbf{r}_S)=\psi(\mathbf{r}_S)$, as it must be to be a valid wave function, but a discontinuity in derivative is permitted.

The expectation value of the Hamiltonian H in the whole space is given by

$$E=\frac{\int_I d\mathbf{r}\,\phi^* H\phi+\varepsilon\int_{II}d\mathbf{r}|\psi|^2+\frac{1}{2}\int_S d\mathbf{r}_S\,\phi^*\left(\frac{\partial\phi}{\partial n_S}-\frac{\partial\psi}{\partial n_S}\right)}{\int_I d\mathbf{r}|\phi|^2+\int_{II}d\mathbf{r}|\psi|^2}, \tag{45}$$

where n_S is the unit vector normal to the infinitesimal surface elements $d\mathbf{r}_S$ pointing out of the region I, and the surface integral term is the kinetic-energy contribution arising from the discontinuity of the wave-function derivative across S. The volume integral in region II may be eliminated by introducing the Green's function G_0 for the unperturbed system, which satisfies a zero normal-derivative boundary condition on S:

$$\frac{\partial G_0(\mathbf{r}_S,\mathbf{r}';\varepsilon)}{\partial n_S}=0. \tag{46}$$

The surface inverse of this Green's function is a generalized logarithmic derivative, which relates the amplitude and derivative of the wave function on surface S:

$$\frac{\partial}{\partial n_S}\psi(\mathbf{r}_S)=-2\int_S d\mathbf{r}'_S\;\; G_0^{-1}(\mathbf{r}_S,\mathbf{r}'_S;\varepsilon)\psi(\mathbf{r}'_S). \tag{47}$$

Following Inglesfield (1981) one can thus obtain the expectation value of the Hamiltonian (usually the Kohn-Sham Hamiltonian) with the trial function, purely in terms of quantities evaluated within or on the surface of region I:

$$E=\left[\int_I d\mathbf{r}\,\phi^* H\phi+\frac{1}{2}\int_S d\mathbf{r}_S\,\phi^*\frac{\partial\phi}{\partial n_S}+\int_S d\mathbf{r}_S\int_S d\mathbf{r}'_S\,\phi^*\left(G_0^{-1}(\varepsilon)-\varepsilon\frac{\partial G_0^{-1}(\varepsilon)}{\partial\varepsilon}\right)\phi\right]\Bigg/$$
$$\left[\int_I d\mathbf{r}|\phi|^2-\int_S d\mathbf{r}_S\int_S d\mathbf{r}'_S\,\phi^*\frac{\partial G_0^{-1}(\varepsilon)}{\partial\varepsilon}\phi\right]. \tag{48}$$

If this equation is minimized with respect to the trial function ϕ, and ε is fixed on the working energy E, one obtains the following Schrödinger equation:

$$\left(H+\frac{1}{2}\delta(\mathbf{r}-\mathbf{r}_S)\frac{\partial}{\partial n_S}\right)\phi(\mathbf{r})+\delta(\mathbf{r}-\mathbf{r}_S)\int_S d\mathbf{r}'_S\,G_0^{-1}(\mathbf{r}_S,\mathbf{r}'_S;E)\,\phi(\mathbf{r}'_S)=E\,\phi(\mathbf{r})\quad\text{with}\quad\mathbf{r}\in I. \tag{49}$$

As one can see from Eq. (49), in this approach one takes into account the effect of the solid via a nonlocal energy-dependent potential (the embedding potential) defined on the surface of the embedded region. This potential acts as a boundary condition on the solution, in contrast to other treatments where the Dyson equation is used (Gunnarsson and Hjelmberg, 1975; Williams, Feibelman, and Lang, 1982; Scheffler *et al.*, 1991) and where the corresponding boundary conditions enter in a basis-set expansion throughout the localized region.

Unlike the approaches of Williams, Feibelman, and Lang (1982) and Scheffler *et al.* (1991), the Green's-function matching technique for a single adsorbate has been applied only to a jellium surface. So, though it is a useful alternative approach to the Dyson equation method, it does not at present display the variety and generality of results of the other methods.

Recent improvements both in numerical facilities and in minimization techniques have made the slab and the supercell methods (Sec. IV.C) an easier route to obtaining the adiabatic electronic properties of an adsorbed molecule, especially for total-energy calculations. For this reason several of the above-mentioned embedding methods have become less popular. However, the embedding method is still valuable in allowing one to consider a truly continuum spectrum of the electronic density of states.

C. The slab and supercell methods

In the slab approach the semi-infinite metal is replaced by a slab with two surfaces. In this way one obtains a 2D lattice, while the problem becomes finite in the direction $\hat{z}$ normal to the surfaces (Inglesfield and Holland, 1981). To deal with the statics of adsorption, a 2D periodic array of molecules is then usually set on one of the two surfaces (te Velde and Baerends, 1993). Hence it is possible to define a 2D periodic unit cell that extends in the $\hat{z}$ direction far enough to include a single molecule of the surface overlayer. For each point $\mathbf{L}$ of the 2D lattice there are several atomic sites $\mathbf{l}_i$—in the simplest case, one atom in each layer of the slab. To calculate the electronic structure of this system, one can use standard basis-set methods, such as the LCAO or tight-binding approach (see Callaway, 1974, p. 292; Inglesfield and Holland, 1981; te Velde and Baerends, 1993), by constructing wave functions that obey Bloch's theorem in 2D as linear combinations of a set of localized orbitals $\{\phi_\alpha\}$ at sites $\mathbf{l}_i$:

$$\psi_{\alpha,i}(\mathbf{r})=N_L^{-(1/2)}\sum_{\mathbf{L}}\,e^{i\mathbf{K}\cdot\mathbf{L}}\phi_\alpha(\mathbf{r}-\mathbf{l}_i-\mathbf{L}). \tag{50}$$

In Eq. (50) $\mathbf{K}$ is a 2D wave vector defined in the 2D first Brillouin zone and N_L the number of 2D periodic unit cells in the system. The exact Bloch wave functions $\Psi_{\mathbf{K}}(\mathbf{r})$ are linear combinations of functions $\psi_{\alpha,i}(\mathbf{r})$:

$$\Psi_{\mathbf{K}}(\mathbf{r})=\sum_{\alpha,i}\,c_{\alpha,i}\psi_{\alpha,i}(\mathbf{r}). \tag{51}$$

We can form matrix elements of the Hamiltonian (for example the Kohn-Sham Hamiltonian) on the basis functions $\{\psi_{\alpha,i}\}$, say $H_{\alpha i,\beta j}$, and we can form elements of the overlap term, say $S_{\alpha i,\beta j}$, respectively. In this way the electronic energies and the expansion coefficients in Eq. (51) can be worked out from the solution of the following finite matrix equation:

$$\sum_{\beta,j}\,(H_{\alpha i,\beta j}-E_{\mathbf{K}}S_{\alpha i,\beta j})c_{\beta,j}=0. \tag{52}$$

If one considers a slab of finite thickness, for a given $\mathbf{K}$, the continuum of bulk states encountered in the Green's-function formalism is replaced by a finite set of discrete energy states $E_{\mathbf{K}}$. In order to obtain an electronic structure representative of a real system, the slab should be sufficiently thick that all relevant quantities are independent of thickness. At the same time, in order to study a single molecule interacting with a metal surface, the molecule overlayer should be as dilute as possible, so that the lateral interactions between adsorbates are negligible. In practical calculations one increases the number N_z of layers of the slab and reduces the coverage θ_S of molecules until convergence of important physical quantities such that the adsorption energy of a single molecule is reached [see also te Velde and Baerends (1993) and Wiesenekker, Kroes, and Baerends (1996)].

As already pointed out, a slab is a 2D periodic array in which there is no periodicity in the direction perpendicular to its two surfaces. A way to recover 3D periodicity is to repeat the slabs, adding a vacuum region in between them, in the $\hat{z}$ direction. Of course such a re-

gion has to be wide enough to avoid interaction between different slabs. In this way one can define a 3D periodic unit cell, the supercell, containing the unit cell of a slab and a vacuum region, which is repeated over all space. This approach was introduced to compute the structure of the Si surface by Schlüter *et al.* (1975) and the jellium-Si interface by Louie and Cohen (1976). More recently, a dilute overlayer of adsorbates has been added to either or both surfaces of each slab to study the molecule-surface interaction in fully periodic 3D systems (Payne *et al.*, 1992). We can write each electronic wave function $\psi_{\mathbf{k}}(\mathbf{r})$, characterized by a Bloch 3D wave vector $\mathbf{k}$, as an expansion in plane waves:

$$\psi_{\mathbf{k}}(\mathbf{r})=N_{sc}^{-(1/2)}\sum_{\mathbf{g}} c_{\mathbf{k}+\mathbf{g},i}e^{i(\mathbf{k}+\mathbf{g})\cdot\mathbf{r}}, \tag{53}$$

where N_{sc} is the number of supercells. The 3D reciprocal-superlattice vectors are defined by

$$\mathbf{g}=\mathbf{G}+2\pi\frac{m}{c}\hat{z}, \tag{54}$$

where m is an integer. In Eq. (54) $\mathbf{G}$ is a 2D reciprocal-lattice vector for an overlayer of molecules on a single slab, and c is the superlattice constant in the $\hat{z}$ direction. Substituting Eq. (53) in the Kohn-Sham equation (10) and integrating over $\mathbf{r}$, such an equation becomes

$$\sum_{\mathbf{g}'}\left(\frac{|\mathbf{k}+\mathbf{g}|^2}{2}\delta_{\mathbf{g}\mathbf{g}'}+v(\mathbf{g}-\mathbf{g}')+V_H(\mathbf{g}-\mathbf{g}')+V_{xc}(\mathbf{g}-\mathbf{g}')-E_{\mathbf{k},i}\delta_{\mathbf{g}\mathbf{g}'}\right)c_{\mathbf{k}+\mathbf{g}',i}=0. \tag{55}$$

In principle an infinite plane-wave basis set is needed to expand the electronic wave function in Eq. (53). In practice, a cutoff in the kinetic-energy term $\frac{1}{2}|\mathbf{k}+\mathbf{g}|^2$, since the plane waves of smaller kinetic energy are more important in the potential-energy terms in Eq. (55), allows one to solve a finite-matrix problem. The cutoff energy should be large enough to ensure convergence of the calculated quantities such as the adsorption energies. A discussion of the activation barrier energy for H_2 dissociation on Cu(111), as a function of the cutoff energy and the number of plane waves, is presented by Hammer *et al.* (1994). Criteria for selecting a special set of wave vectors $\mathbf{k}$ within the first Brillouin zone also exist (Payne *et al.*, 1992).

In conclusion, the supercell method requires a larger plane-wave basis set than the localized basis set of the slab approach, if we take into account either 3D or 2D periodic unit cells, respectively, containing a few atoms. However, matrix elements on plane waves are usually easier to compute, while the matrix dimension of the slab approach increases rapidly as soon as a good number of atoms are included in the system to avoid interaction between adsorbates. Within the framework of the slab approach, it has been shown that for the system CO/Cu(100) the adsorption energy E_{ads}, as a function of N_z and θ_S, exhibits good convergence. In fact, $N_z=3$ and $\theta_S=\frac{1}{2}$ are sufficient to obtain fairly stable results. This contrasts with the oscillatory behavior of the calculated E_{ads} for the same system, which one observes by increasing the number of atoms in a cluster approach. For a detailed comparison of the two methods see te Velde and Baerends (1993).

V. THEORETICAL ISSUES

A. Quantities of physical interest

Both in the self-consistent solution of the Kohn-Sham equation and as a quantity of physical interest, the electron charge density $\rho(\mathbf{r})$ plays a major role in adsorption theory. In the most elegant way, one makes use of the Green's-function formalism and defines the charge density from the local density of states (LDOS) $\rho(\mathbf{r},E)$, given by

$$\rho(\mathbf{r},E)=\frac{1}{\pi}\mathrm{Im}\,G(\mathbf{r},\mathbf{r};E+i\epsilon), \tag{56}$$

where $i\epsilon$ is a small imaginary energy. Making use of the wave function $\psi_i(\mathbf{r})$ solutions of an effective single-particle Schrödinger equation, one can write the LDOS as

$$\rho(\mathbf{r},E)=\sum_i \psi_i(\mathbf{r})^*\psi_i(\mathbf{r})\,\delta(E-E_i). \tag{57}$$

The charge density is found by integrating Eq. (56) up to the Fermi energy E_F. This is most economically performed by contour integration, exploiting the analyticity of the Green's function in the upper half plane:

$$\rho(\mathbf{r})=\frac{1}{\pi}\mathrm{Im}\int_c dz\;\; G(\mathbf{r},\mathbf{r};z), \tag{58}$$

with the curve c beginning below the lowest occupied state and returning to the real energy axis at the Fermi energy E_F. When the spectrum is discrete, as in the slab and supercell or in cluster calculations, after integrating over the energy up to E_F in Eq. (57), one obtains

$$\rho(\mathbf{r})=\sum_{i\in\mathrm{occ}} \psi_i(\mathbf{r})^*\psi_i(\mathbf{r}). \tag{59}$$

If the system is defined by a many-particle wave function one can define the charge density $\rho(\mathbf{r})$ from the first-order density matrix [Eqs. (22) and (23)].

The density of states (DOS) is found from the spatial integral of the LDOS:

$$\rho(E)=\int_{\mathcal{V}} d\mathbf{r}\,\rho(\mathbf{r},E), \tag{60}$$

a result which clearly depends upon the integration volume $\mathcal{V}$. The induced DOS, $\Delta\rho_{\mathcal{V}}(E)$, is defined as the difference between the DOS of the molecule-metal system and the DOS of the bare substrate. In this way, if a finite system adsorption calculation is performed, one can obtain the induced DOS from the DOS. On the other hand, the embedding approach implies a semi-infinite substrate ($\mathcal{V}\to\infty$) where the integral in Eq. (60) diverges. Note that such an integral has to be computed

explicitly, since changes in $\rho(\mathbf{r},E)$ due to adsorption throughout the whole space should be considered. But it can be shown that by using the generalized phase shift method one can access the induced DOS $\Delta\rho(E)$ in the localized plus the extended substrate. See also Eqs. (65), (66), and (67) below.

The projected LDOS, often also called the projected DOS, on a specific orbital $\phi(\mathbf{r})$ is given by

$$\rho_\phi(E)=\sum_i |\langle\phi|\psi_i\rangle|^2\delta(E-E_i). \tag{61}$$

Finally, we discuss the total energy of the system and, in particular, the interaction energy $\mathcal{E}(\mathbf{R})$ of a molecule with the surface. Here, in contrast to an atom-surface system, $\mathbf{R}$ denotes a generalized coordinate for a molecule. This interaction energy is given by the difference between the total energy of the interacting system $E_{\text{surf+mol}}$ and the reference energies of the clean surface E_{surf} and the isolated molecule E_{mol}:

$$\mathcal{E}(\mathbf{R})=E_{\text{surf+mol}}(\mathbf{R})-E_{\text{surf}}-E_{\text{mol}}. \tag{62}$$

Note that $\mathcal{E}(\mathbf{R})$ represents the adiabatic molecule-metal potential-energy surface derived in an *ab initio* framework, which is otherwise denoted by $V(\mathbf{R})$ in this article. To compute the various terms in Eq. (62), one can write the total energy of an interacting ensemble of electrons as

$$E=\langle T\rangle+\langle U\rangle+E_{xc}, \tag{63}$$

where $\langle T\rangle$ is the kinetic-energy contribution, $\langle U\rangle$ is the classical Coulomb interaction, and E_{xc} is the exchange-correlation energy. Within the framework of the density-functional theory such terms have been discussed in Sec. III. The kinetic energy can be determined using the sum of eigenvalues of the effective Schrödinger equation, e.g., the Kohn-Sham Hamiltonian in Eq. (10):

$$\langle T\rangle=\sum_{i\in\text{occ}}\varepsilon_i-\int d\mathbf{r}\, v_{\text{eff}}(\mathbf{r})\rho(\mathbf{r}). \tag{64}$$

Note that in the calculation all energy differences refer to quantities obtained within the region where the molecule-metal electronic properties are explicitly calculated, except in the embedding approach. Here consider the so-called band-structure energy term obtained from the eigenvalue perturbation:

$$\Delta E_{\text{band}}=\int_{-\infty}^{E_F} dE\, E\Delta\rho(E). \tag{65}$$

This term, in the generalized phase-shift method (Inglesfield and Benesh, 1988b), can take into account changes in the induced DOS in the whole space, due to the presence of the adsorbate. From Eq. (65) one can write the band-structure contribution, ΔE_{band}, as

$$\Delta E_{\text{band}}=E_F\Delta N(E_F)-\int_{-\infty}^{E_F} dE\,\Delta N(E). \tag{66}$$

In Eq. (66) $\Delta N(E)$ is the change in the number of states induced by the impurity up to the energy E in the whole system (see Callaway, 1974, p. 435), which can be expressed in terms of the induced DOS $\Delta\rho(E)$ by

$$\Delta N(E)=\int_{-\infty}^{E} dE'\,\Delta\rho(E'). \tag{67}$$

Note that Eq. (67) also supplies the definition of $\Delta\rho(E)$.

B. The Friedel sum rule

The concepts outlined in this section are more generally valid for any impurity in a host, so that an admolecule is a particular case.

Consider an adsorbate interacting with a semi-infinite substrate, which fixes the Fermi energy of the system. Label the impurity positive charge $\mathcal{Z}$. We expect the charge $\mathcal{Z}$ to affect the electronic charge distribution of the system, which will rearrange to screen the defect Coulomb potential at large enough distances from the adparticle. Call I the region where the adsorption calculation is worked out, and $\mathcal{V}_I$ its volume. If the perturbation is localized within the region I, charge neutrality is still retained. Hence it follows that

$$\int_{\mathcal{V}_I} d\mathbf{r}\,\Delta\rho(\mathbf{r})=\mathcal{Z}. \tag{68}$$

At the same time the so-called Friedel's sum rule (Callaway, 1974), holds that

$$\Delta N(E_F)=\mathcal{Z}. \tag{69}$$

Obviously the results of Eqs. (68) and (69) are always valid for $\mathcal{V}_I\to R^3$, i.e., the localized region coinciding with the whole space.

However, if the perturbation, which may, for example, induce Friedel's oscillations in a metal, is not localized in $\mathcal{V}_I$, an excess or deficit of the electronic charge will show up not only in $\mathcal{V}_I$ but in the whole space, from the calculated results. Consequently Eqs. (68) and (69) are no longer valid. Note also that generally the resulting charge from Eqs. (68) and (69) will not be the same. In fact Eq. (68) calculates a charge Q_{loc} and hence an excess/deficit of electronic charge $\Delta Q_{\text{loc}}=Q_{\text{loc}}-\mathcal{Z}$ in the region $\mathcal{V}_I$. Equation (69) calculates a charge Q and an excess/deficit $\Delta Q=Q-\mathcal{Z}$ in the entire region. The excess or deficit of charge is an unphysical artifact of the lack of total screening in the system, since we are working in too small a region.

The knowledge of ΔQ has two important consequences: (a) Together with the local excess or deficit of charge ΔQ_{loc} it allows us to estimate how good our choice of the local region I is; (b) If we recall that the only term in the adsorption energy, which contains information on the effect of the perturbation in the whole space, is the band structure, via ΔQ, we can introduce a meaningful correction to ΔE_{band}, as we shall now discuss [see Eq. (66)].

We follow a treatment proposed by Drittler *et al.* (1989). Consider the total-energy functional $E[\rho(\mathbf{r})]$ of an impurity in a host. It is well known that $E[\rho(\mathbf{r})]$ is a

functional of the trial charge density $\rho(\mathbf{r})$ and hence is extremal against charge variations $\delta\rho(\mathbf{r})$ around the ground state:

$$\delta E = \int d\mathbf{r}\, \frac{\delta E}{\delta \rho}\, \delta\rho(\mathbf{r}) = E_F \int d\mathbf{r}\, \delta\rho(\mathbf{r}). \tag{70}$$

δE vanishes if $\int d\mathbf{r}\, \delta\rho(\mathbf{r}) = 0$. This result is valid as long as $\rho(\mathbf{r})$ gives the correct charge of the system:

$$\mathcal{Z} = \int d\mathbf{r}\, \Delta\rho(\mathbf{r}). \tag{71}$$

However, as already pointed out, charge neutrality may be violated if the perturbation potential of the impurity is not fully included in the calculation, as occurs in all adsorption problems, since Friedel's oscillations display a long-range character (Lang and Williams, 1978). This may be avoided if the generalized functional $\tilde{E}[\rho(\mathbf{r})]$ is introduced:

$$\tilde{E}[\rho(\mathbf{r})] = E[\rho(\mathbf{r})] - \Delta E_{\mathrm{G.C.}}$$

$$\Delta E_{\mathrm{G.C.}} = E_F \left(\int d\mathbf{r}\, \Delta\rho(\mathbf{r}) - \mathcal{Z} \right). \tag{72}$$

Clearly $\delta\tilde{E} = 0$ for general (and non-charge-conserving) variations of $\delta\rho(\mathbf{r})$. Physically, via Eq. (71), we take into account a new grand canonical functional, which fixes the chemical potential E_F but not the number of particles, i.e., their charge $\mathcal{Z}$. This is a first-order correction to the energy E in which the excess/missing charge ΔQ is added at the Fermi level of the host, giving an additional energy contribution $E_F \Delta Q$.

The grand canonical correction to the total energy of an impurity in the bulk is usually negligible in most calculations (Drittler *et al.*, 1989). Owing to the much lower symmetry of an adsorbate, it produces a much larger correction. A discussion of the grand canonical correction to the chemisorption energy of adatoms is presented in Sec. VII. It is, however, instructive to estimate its contribution to the interaction energy of a He atom on an (Ag-like) jellium surface within a density-functional-LDA calculation with the Green's-function matching technique (Trioni *et al.*, 1998). This is because, although here the magnitude of ΔQ is fairly small, as it spans from 0 to 2.5×10^{-2} electrons by varying the He distance Z from the jellium edge, the grand canonical correction is essential to give the right behavior of the adsorption curve. The broken line in Fig. 4 shows the He-jellium adiabatic potential $\mathcal{E}(Z)$ calculated by the functional in Eq. (62), which is wrong. The solid line displays the correct $\mathcal{E}(Z)$ calculated by the grand canonical functional in Eq. (72). The inset shows ΔQ. Being the calculation performed in the density-functional-LDA framework, $\mathcal{E}(Z)$ is most adequately reproduced in the repulsive region.

Finally we write down the adsorption energy contribution of the band term in the grand canonical framework:

$$\Delta\tilde{E} = \Delta E_{\mathrm{band}} - \Delta E_{\mathrm{G.C.}} = E_F \mathcal{Z} - \int_{-\infty}^{E_F} dE\, \Delta N(E). \tag{73}$$

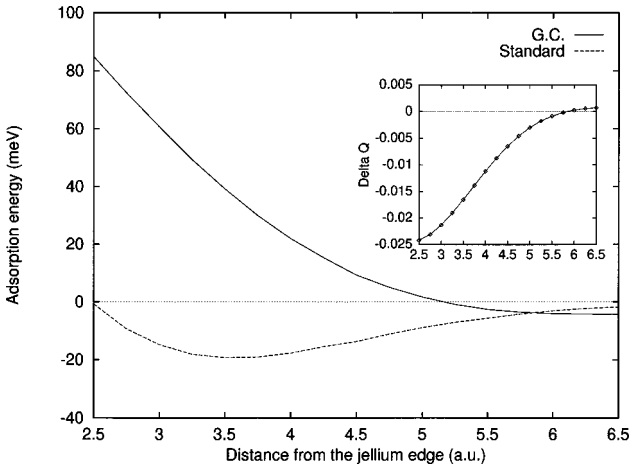

FIG. 4. He-jellium (Ag-like) potential as a function of the distance from the jellium edge: dashed line, from a calculation by Eq. (62); solid line, from a calculation by Eq. (72). The inset shows the defect of electronic charge in the whole system as function of Z. For details see the text.

Consider next a calculation within the cluster or the slab/supercell method. Here the charge is automatically conserved. The output is a discrete set of levels, the last occupied one being the Fermi level, which may undergo a small variation $E_F \rightarrow E_F + \delta E_F$ after introducing the impurity. Then, if we take advantage of the charge neutrality and determine δE_F from it, the band-structure contribution in Eq. (65) becomes

$$\Delta E_{\mathrm{band}} = \int_{-\infty}^{E_F + \delta E_F} dE\, E\Delta\rho(E) = E_F \Delta N(E_F) - \int_{-\infty}^{E_F} dE\, \Delta N(E) + E_F[\mathcal{Z} - \Delta N(E_F)]. \tag{74}$$

Equation (74) is exactly the grand-canonical result. So, if the neutrality condition is imposed, one has to allow for the Fermi energy to vary upon adsorption. In this way, the grand-canonical result is achieved in a finite system.

VI. PHYSISORPTION

The main goal of physisorption theory of noble gases on metals is to obtain the particle-surface interaction in a unified approach valid at any distance of the atom from the surface. In principle this could be obtained within the density-functional formalism. By using this formalism, it has been shown that, if one is able to work out a unified theory that gives the correct asymptotic image potential of a clean metal surface (Zangwill, 1988), the van der Waals potential between a neutral atom and the surface is recovered (Annett and Haydock, 1986).

In practice, however, the usual difficulty lies in obtaining the nonlocal response function of the metal defined by

$$\chi(\mathbf{r},\mathbf{r}';\omega) = \frac{i}{2\pi} \int_0^\infty dt\, e^{i\omega t} \langle [\hat{n}(\mathbf{r},t), \hat{n}(\mathbf{r}',0)] \rangle, \tag{75}$$

where $\hat{n}(\mathbf{r},t)$ is the density operator for an electron at position $\mathbf{r}$ and time t. The bracketed quantity is the ground-state expectation value of the indicated commutator. A recent attempt to obtain the nonlocal response function via a local approximation of the dielectric function of the metal is that of Hult *et al.* (1996) and Hult and Kiejna (1997). Modifications to the Zaremba-Kohn theory have been made that, by introducing a certain self-consistency into the response of the solid to an external charge, affect the formula for the reference plane position Z_0, leading to smaller values in general.

However, Eq. (75) has not yet been evaluated beyond the local-density approach. This is still an open and important question because the correct van der Waals behavior of the gas-metal potential affects both the amplitudes of light noble-gas probes scattering off metals (Karikorpi, Manninen, and Umrigar, 1986) and dynamical quantities such as sticking coefficients and desorption rates (Brivio *et al.*, 1993).

The difficulty of calculating *ab initio* the physisorption potential of a noble gas interacting with a metal surface has led several authors, as already pointed out in Sec. II, to compute the potential closer to the surface, and to add the van der Waals part later (Harris and Liebsch, 1982; Chizmeshya and Zaremba, 1992). Note that, to obtain the minimum of the physisorption potential, the van der Waals interaction has to be added if the approach is only capable of obtaining the repulsive part (Kohn, 1990). In some other approaches, such as the density-functional–LDA, a reasonable physisorption well can be obtained (Lang, 1981; Lang and Nørskov, 1983), though the calculated potential does not display the correct van der Waals tail, but it drops to zero too quickly. This is because the LDA can readily account for a phenomenon such as the Pauli repulsion experienced by a noble-gas atom very close to the metal. Lang (1981), in his work on jellium, has shown that the LDA may provide a good account of the adatom binding energy. An intuitive explanation of this effect is related to the fact that, at such atom-surface distances, it is correct to consider the electron to be attached to its exchange-correlation hole, as in the LDA.

We now review the most important papers on the theory of physisorption of noble gases on metals since 1980, outlining results and open problems.

A. The effective-medium theory

In 1980 Nørskov and Lang (1980) introduced the effective-medium theory. This method simplifies the particle-surface problem by replacing the surface by a uniform medium simulating the metal's electronic tail. In other words, the atom is embedded in a homogeneous electron gas of density $\overline{\rho}_R$, where $\overline{\rho}_R$ is an average of the unperturbed charge density $\rho_M(\mathbf{r})$ of the surface in the adatom region (see also Stott and Zaremba, 1980). Such an average is weighted on the potential induced by the unperturbed atom:

$$\overline{\rho}_R = \frac{\int d\mathbf{r}\, \rho_M(\mathbf{r}) \Delta\phi_R(\mathbf{r})}{\int d\mathbf{r}\, \Delta\phi_R(\mathbf{r})}, \tag{76}$$

$$\Delta\phi_R(\mathbf{r}) = \int d\mathbf{r}' \frac{\Delta\rho(\mathbf{r}') - \mathcal{Z}\delta(\mathbf{r}'-\mathbf{R})}{|\mathbf{r}-\mathbf{r}'|}. \tag{77}$$

Note that $\overline{\rho}_R$ and $\Delta\phi_R$, which is the potential induced by the atom considering its positive and negative charges, depend on the distance $\mathbf{R}$ of the atom from the surface.

At zero order in the perturbation potential induced on the atom by the surface, one can define an embedding energy $\Delta E^{\mathrm{hom}}(\overline{\rho}_R)$ of the atom in a homogeneous jellium of density $\overline{\rho}_R$. This approximation represents the main result of the effective-medium theory, since it allows one to work out molecule-surface energies, and for this reason it has motivated several applications beyond physisorption, e.g., it has also been applied to chemisorbed systems (see, for example, Nørskov, 1982; Raeker and DePristo, 1990).

Esbjerg and Nørskov (1980) showed that for a weak atom-metal interaction (with closed-shell atoms) it is possible, via the embedding energy, to arrive at a very simple expression for the atom-surface potential, which is only a repulsive energy V^{rep}:

$$V^{\mathrm{rep}}(\mathbf{R}) = \Delta E^{\mathrm{hom}}(\overline{\rho}_R) \simeq \alpha_{\mathrm{eff}} \overline{\rho}_R. \tag{78}$$

In the original paper (Esbjerg and Nørskov, 1980) the averaging procedure that leads to $\overline{\rho}_R$ is replaced by the value of the unperturbed charge density $\rho_M(R)$, and the proportionality constant, say α to distinguish it from α_{eff}, which takes into account some surface effects, is derived by a fitting procedure.

Several authors have endeavored to obtain the most physical values for α and α_{eff}. This effort has produced an ample literature on the subject, to which the interested reader is referred (Puska, Nieminen, and Manninen, 1981; Manninen *et al.*, 1984; Cole and Toigo, 1985; Karikorpi, Manninen, and Umrigar, 1986). If we concentrate on the simpler coefficient α just defined, a consensus currently exists that the value for He is slightly larger than 300 eV a_0^3 (Manninen *et al.*, 1984; Cole and Toigo, 1985).

The success of the effective-medium theory at the time it was formulated was based on two factors: first, its ability to obtain adsorption energies by a simple scheme, and second, its ability to avoid prohibitive calculations since numerical complications arise as soon as the lattice properties of the system are considered. However, it was soon realized that tests to check the results of the effective-medium theory were necessary. For this reason Lang and Nørskov (1983) presented a comparison between the effective-medium theory, including an attractive atom-surface potential, and a density-functional–LDA calculation, within the framework of the method developed by Lang and Williams (1978) for the He-metal (jellium with $r_s=3$) potential-energy surface. More exactly, they refined the effective-medium result and calculated the atom-surface interaction energy by taking into account the deviation of the surface electron density from homogeneity in first-order perturbation theory. They verified that the *ab initio* results and the effective-medium results are of the same order of mag-

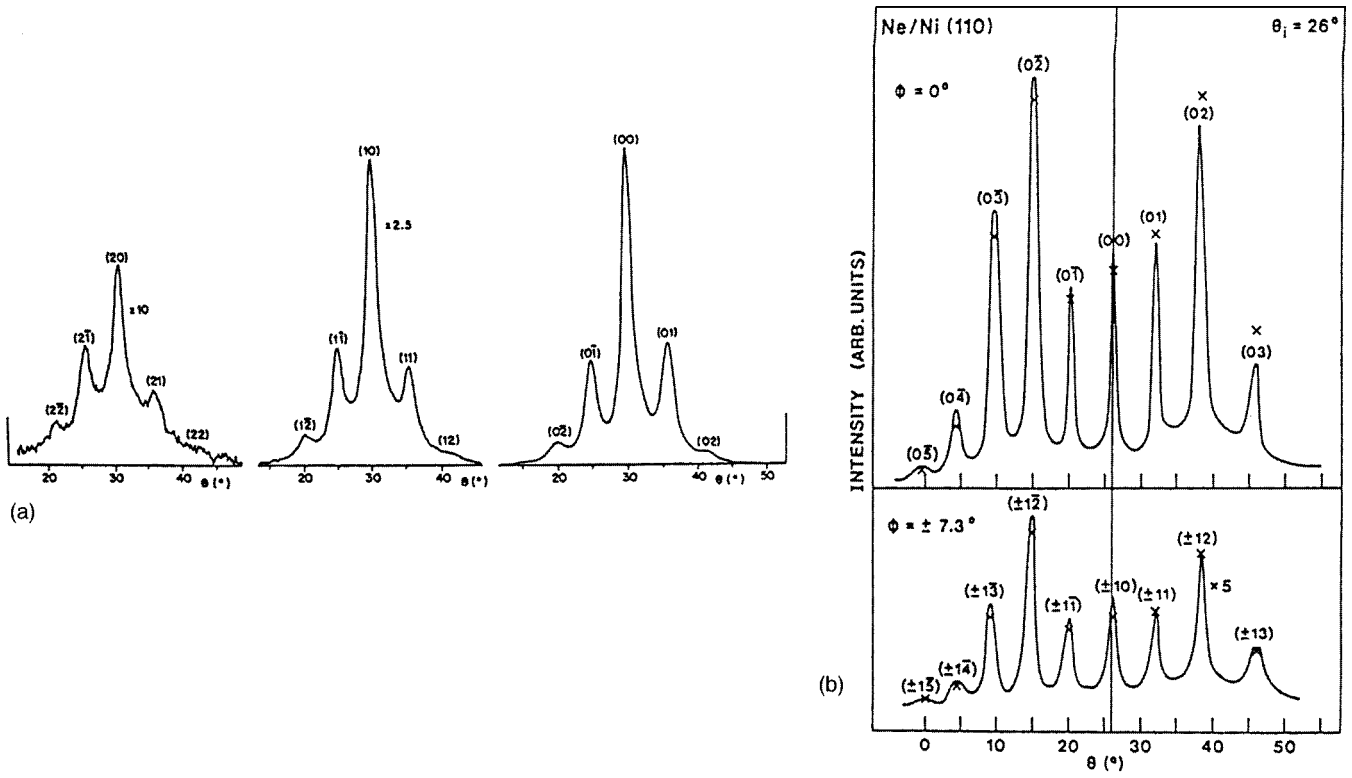

FIG. 5. Diffraction spectra from Ni(110). (a) From right: first spectrum, in-plane ($\phi=0°$); last two spectra, out-of-plane ($\phi=\pm 6.4°, \pm 12.9°$) diffraction spectra from Ni(110) of a He beam with energy $E_i=266$ meV and $\theta_i=30°$. Note that θ_i labels the polar angle and ϕ the azimuthal angle with respect to the surface normal, respectively. (b) Diffraction spectra obtained with a Ne atomic beam from Ni(110). Note a pronounced rainbow near the (0 ± 2) beams, indicating a larger corrugation amplitude observed with Ne than with He. From Rieder (1994).

nitude, but that the He-metal potential-energy curve, computed by the effective-medium theory, is significantly smaller at shorter atom-surface distances. Moreover, the physisorption well obtained by the effective-medium theory is too shallow.

Harris and Liebsch (1982) presented a generalization of the Zaremba-Kohn treatment for the repulsive part of the physisorption potential. They considered a density-functional approach, in which the atom-metal correlation was ignored. By adding the van der Waals contribution $V_{\rm corr}$ they were able to write down a useful formula for the particle-metal interaction, to first order in the overlap between the metal and the particle

$$V(Z)=\sum_k \Delta\varepsilon_k + V_{\rm corr}(Z), \tag{79}$$

where $\Delta\varepsilon_k$ is the change in the metal eigenvalues due to particle perturbation. Harris and Liebsch also proved that the average density method proposed by Esbjerg and Nørskov (1980) [see Eq. (78)] is valid only on a jellium surface (translationally invariant for any 2D vector). Such a simplification cannot account for anticorrugating effects (see the following), since in Esbjerg and Nørskov (1980) the atom-surface potential profile is always proportional to the charge distribution.

B. He and Ne physisorption

Now let us consider two effects recently derived from experiments in which He and Ne were scattered off metals.

The first effect was reported by Rieder and Stocker (1984) and Salanon (1984). They observed in separate scattering experiments with low-energy atoms that Ne was much more sensitive to the details of the corrugation of a metal surface than the more commonly used He atom. Note that the corrugation profile depends on the impinging atom's kinetic energy. The results of Rieder and Stocker (1984) are shown in Fig. 5. In those diffraction spectra Ne displays a stronger rainbow effect (Celli, 1984), which indicates a much larger corrugation amplitude for Ne than that for He, the probes scattering off Ni(110). The same qualitative findings were obtained for He and Ne on Cu(110) by Salanon (1984). A more detailed analysis of the diffraction pattern gives a corrugation amplitude "seen" by Ne about twice as that by He. To interpret these results, the corrugation function $\zeta(\mathbf{R}_\parallel)$, representing the classical turning point as a function of $\mathbf{R}_\parallel\equiv(X,Y)$, and defined in Sec. II.B, is builtup by fitting some parameters [$z(10)$ and $z(01)$] in Eq. (80). In this way one can reproduce the intensity of the experimental peaks by solving a coupled-channels equation (Celli, 1984). Figure 6 shows the function ζ used by Rieder and Stocker (1984), given by

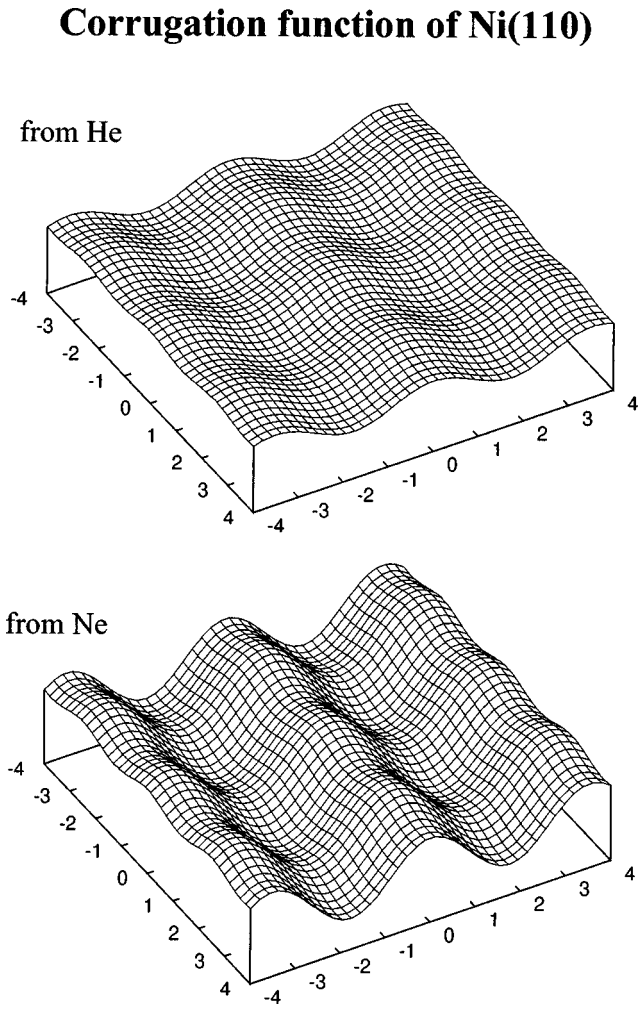

FIG. 6. Corrugation function of He (upper panel) and Ne (lower panel) on Ni(110).

$$\zeta(X,Y)=1/2[z(10)\cos(2\pi X/a_1)+z(01)\cos(2\pi Y/a_2)], \tag{80}$$

where a_1 and a_2 are the 2D surface lattice constants. Values for Ni(110), as seen by atomic beams of He and Ne, are $a_1=2.49$ Å, $a_2=3.52$ Å, $z(10)_{\mathrm{He}}\sim 0.017$ Å, $z(01)_{\mathrm{He}}=0.075$ Å, $z(10)_{\mathrm{Ne}}=0.033$ Å, $z(01)_{\mathrm{Ne}}=0.174$ Å. On the basis of the effective-medium theory, i.e., the hypothesis that the potential in the repulsive region can be taken proportional to the electronic charge tail outside the metal, the more corrugated the potential, the more corrugated the charge density. Hence the closer to the surface is the region sampled by the gas atom (see Fig. 7). Looking at the values of the parameters α in Puska *et al.* (1981) and Cole and Toigo (1985) we expect a more pronounced repulsive potential for Ne than for He, at the same incoming particle energy, contrary to the experimental evidence.

Although phenomenological models have been proposed (Salanon, 1984; Cvetko *et al.*, 1994), this is a clear case in which *ab initio* results should be worked out in order to pinpoint the discrepancy between the effective-medium theory and the experimental results. A calculation of the adiabatic electronic properties of an isolated

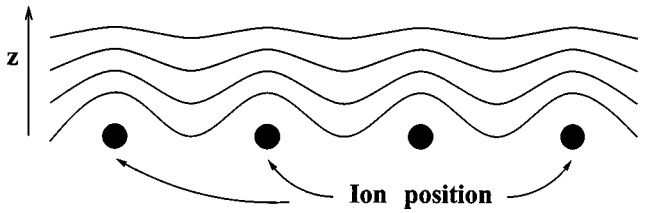

FIG. 7. Schematic example of the charge profile of a clean metal surface. Near the uppermost ion row the charge corrugation is higher than in the far region.

He and Ne atom on a metal from first principles has been proposed by Montalenti *et al.* (1996). Though the substrate is limited to jellium, with no lattice structure, this is still expected to be a useful model for dealing with general properties of the atom-metal surface interaction. Montalenti *et al.* (1996) report on an *ab initio* calculation of the adiabatic electronic properties of He and Ne atoms interacting with a jellium surface (Al-like with $r_s=2.07$) in the framework of the embedding method (Trioni *et al.*, 1996) and using a density-functional–LDA approach. This work focused on the atom-surface region where the potential was repulsive. For incident atoms with the same initial kinetic energies in the typical experimental range (up to about 200 meV), it was shown that Ne got closer to the metal than He. Figure 8 shows the potential-energy curves $\mathcal{E}(Z)$ for He and Ne on Al as a function of Z in the region where repulsive effects

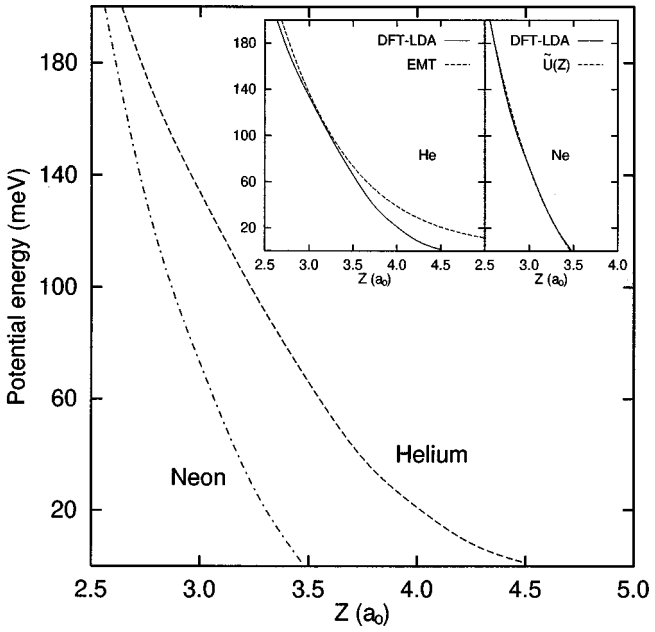

FIG. 8. The potential energies (meV) for single atoms of He (dashed line) and Ne (dot-dashed line) atom, on Al-like jellium surface, as a function of the atom-jellium edge distance (in units of a_0). Left inset the same for He (solid line, the density-functional–LDA result; dashed line, the effective-medium theory result). Right inset: the same for Ne (solid line, the density-functional–LDA result; dashed line, the effective-medium result where an attractive potential is added). From Montalenti *et al.* (1996).

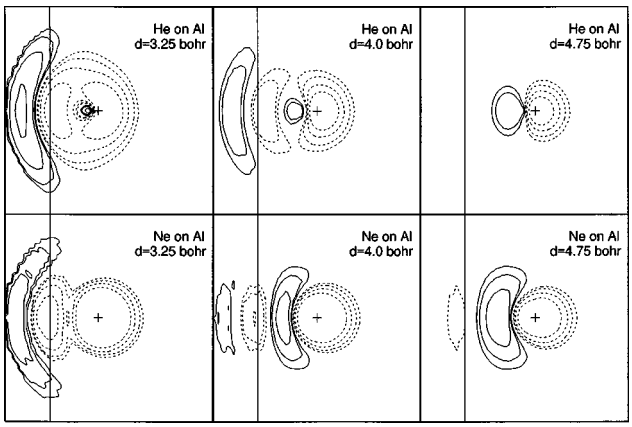

FIG. 9. Contours of the charge displacements (total minus superposition of atomic and bare-metal electron densities): (upper row) a He atom impinging on the Al-jellium surface at three different distances: left panel, $3.25a_0$ (Bohr radius); central panel, $4.0a_0$; right panel, $4.75a_0$; (lower row) the same but for a Ne atom. Contour values shown are ± 0.001, ± 0.0005, ± 0.0003, ± 0.0001 electrons/a_0^3. The cross denotes the adatom nucleus position. The solid line refers to positive excess charge, the dashed line to a negative excess charge. From Montalenti *et al.* (1996).

are dominant. As can be clearly seen, Ne penetrates deeper into the surface electron cloud than He for impinging atom energies in the experimental range. Such a result, which is in agreement with the experiments, can be accounted for in terms of total charge rearrangement, a combined effect due to a larger Pauli repulsion and a more pronounced attraction of the Ne-metal system (because of its larger polarizability) than of the He-metal system. In fact, the p electrons of Ne are not as rigid as the $1s$ electron density of He. From Fig. 8 one can also see that the repulsive potential for He is less steep (softer) than that for Ne, as stated by Rieder and Stocker (1984). In Fig. 9 the total charge rearrangements, both for He and for Ne, are shown at three distances Z.

C. The anticorrugating effect

The second effect was reported by Rieder, Parschau, and Burg (1993). In their very accurate diffraction experiment a surprising behavior was emphasized, namely, that the corrugation profile revealed by He scattering off the surface is translated half the interatomic distance with respect to that obtained by Ne diffraction, i.e., He got closer to the top position than to the bridge one. This behavior is now commonly called the ''anticorrugating effect'' of He.

A theoretical suggestion of this result can be found in earlier work by Annett and Haydock (1984, 1986), where a correction to the Esbjerg and Nørskov (1980) potential energy is proposed to improve the effective-medium theory. Annett and Haydock (1984) note that there is only qualitative agreement between the effective-medium theory and experimental He scattering results (Rieder and Garcia, 1982). For this reason they add two terms to Eq. (78) that solve some discrepancies with the experimental results, essentially due to the overestimate of the corrugation profile given by the effective-medium theory. One needs a contribution that smoothes the corrugation of the effective-medium theory, in practice an anticorrugating contribution:

$$V^{\mathrm{rep}}(\mathbf{R}) = \alpha\rho_0(\mathbf{R}) + \beta\nabla^2\rho_0(\mathbf{R}) - \nu\rho_u(\mathbf{R}). \tag{81}$$

In Eq. (81) the term $\beta\nabla^2\rho_0(\mathbf{R})$ (where the parameter β is larger than zero) has been included to allow for the fact that the $1s$ orbital of He has a finite size. This term cannot, however, explain any anticorrugating contribution. Considering $\nu > 0$ as an adjustable parameter for each surface, a much better correspondence with experimental results can be obtained by adding the third term, where $\rho_u(\mathbf{R})$ is the local density of unoccupied metal states at the atomic position $\mathbf{R}$. Annett and Haydock suggest that this last term, which is always an attractive one, is the contribution due to hybridization between the He $1s$ orbital and the unoccupied metal states. In this context ν represents the matrix element of the perturbation induced by the He potential between a $1s$ orbital and empty metal states over an energy denominator.

We return now to the experiments of Rieder, Parschau, and Burg (1993) on He and Ne scattering from Ni(110) and Rh(110). We recall that H atoms are placed in rows along the $[0\bar{1}1]$ direction on the surface, and they are always ''seen'' by the probes as having the largest corrugation amplitude. In other words, the H atoms are used to identify the position of the lattice atoms, in order to relate the maxima of the corrugation profiles either to the top or to the bridge positions. The results shown in Fig. 10 display opposite corrugations for lattice atoms probed by He and Ne atom scattering. Observe that the maximum of the corrugation $\zeta(\mathbf{R}_\parallel)$ for He is in the bridge position, while that for Ne is in the top. To interpret these results Rieder makes use of the Annett and Haydock (1984) model. He argues that the unoccupied metal states are essentially antibonding and have little weight between the surface atoms. Rieder points out that for He the $1s$ orbital has a significant overlap with the antibonding metal states at the top position and negligible overlap at the bridge position. Consequently, the third term dominates in Eq. (81) and anticorrugating behavior occurs, since the He atom gets closer at the top position. This means that the corrugation profile seen by He is off phase with respect to the lattice atom positions. On the other hand, for Ne, owing to parity, the $2p_x$ orbital has a vanishing overlap with the metal antibonding state in the top position and a significant overlap at the bridge position (see Fig. 11). Because of the opposite contributions of the $2s$ and $2p_x$ orbitals, it follows that $-\nu\rho_u(\mathbf{R}) \simeq 0$. For this reason the atom-metal potential $V^{\mathrm{rep}}(\mathbf{R})$ is in phase with the metal, and there are no anticorrugating effects.

Though simple and qualitatively attractive, the explanation just outlined and proposed by Rieder is dubious, as it considers only antibonding metal orbitals, whereas, following Annett and Haydock, one should take into ac-

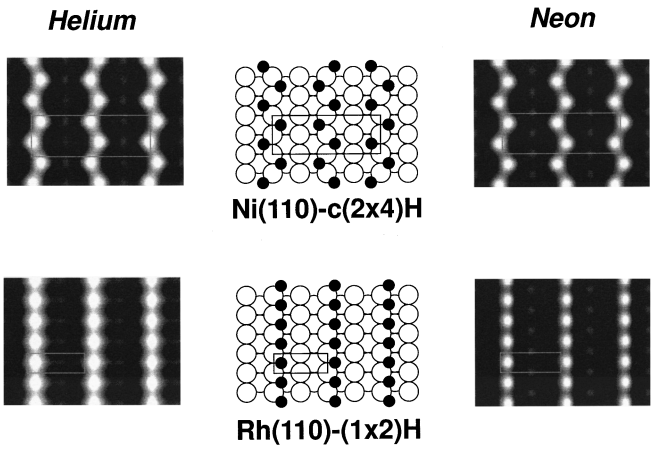

FIG. 10. Sphere models of H phases on Ni(110) and Rh(110) with the grey-scale representations of the corrugation functions derived from He and Ne diffraction: upper row, Ni(110)c (2×4) H; lower row, Rh(110)(1×2)H. ○, metal atoms; ●, H adatoms. The H atoms have the largest corrugation amplitudes and thus show up as the brightest spots. Note that in the He derived corrugations fewer bright maxima occur between the H atoms along the [001] direction on all the H free metal rows, in disagreement with the true atom arrangements. In contrast to this, the Ne derived corrugations are in agreement with the true surface structures. From Rieder *et al.* (1993).

count the full set of unoccupied orbitals. Therefore it is expected that *ab initio* calculations of the interaction potential between a He or Ne atom and a metal surface should provide a firmer background for interpreting the experimental scattering results on the anticorrugating effect. Petersen *et al.* (1996), by using a density-functional–GGA approach and a supercell geometry, have calculated the interaction potential-energy curves for both He and Ne along the top and the short bridge positions of a Rh(110) surface. Their results in Fig. 12 show that He gets closer to the surface at the top than at the bridge position, while the opposite occurs for Ne, in agreement with Rieder's results. The physical interpretation of these phenomena involves a detailed analysis of the hybridization between the noble-gas orbitals and the *d*-band states of the metal. Consequently the anti-

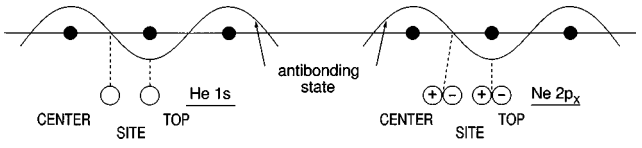

FIG. 11. Rieder's (Rieder *et al.*, 1993) explanation of the anticorrugating effect. Left side: the He 1*s* orbital shows strong overlap with the unoccopied metal states at top positions, whereas the overlap is zero at bridge positions. This (see the text) leads to an anticorrugating effect. Right side: for Ne the $2p_x$ orbital shows no interaction with the unoccupied metal state at top sites, but there is a strong overlap at bridge sites where both the $2p_x$ and metal orbitals change sign. Hence there is a much smaller anticorrugating contribution than in the case of He.

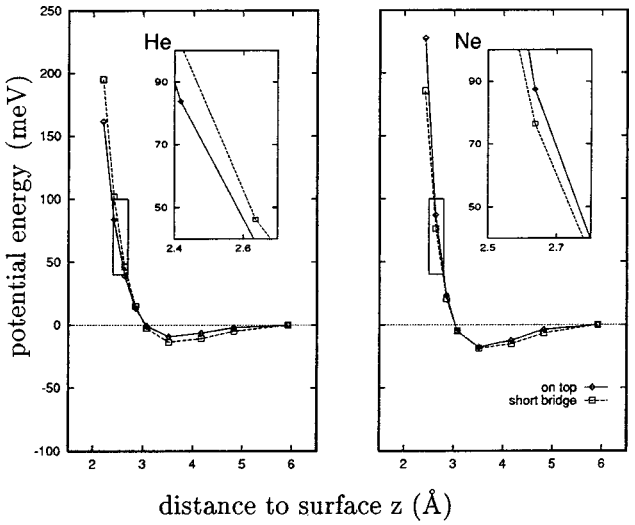

FIG. 12. Calculated potential energy using a density-functional–GGA for a He atom (left) and a Ne atom (right) approaching the top and short-bridge positions of Rh(110) as a function of the distance Z (Å) from the center of the first surface layer. The insets show a magnification of the repulsive part of the potential within the kinetic-energy range used in experiments. From Petersen *et al.* (1996).

corrugating effect of He may not be present for metals with a different band structure.

In the framework of the embedding method and using a density-functional–LDA, a different point of view is proposed by Trioni, Montalenti, and Brivio (1998). They show how the different polarization of He with respect to Ne, induced by the interaction with a simple (jellium) metal, could account for an anticorrugating contribution to the potential energy.

Finally, we wish to comment on the penetration problem of He and Ne and anticorrugating effects. From the theoretical results (Montalenti *et al.*, 1996; Petersen *et al.*, 1996) computed for very different systems, one cannot conclude that the corrugation seen by Ne corresponds to a larger penetration of Ne than of He (at the same incoming particle energy). Observe that in the calculations by Petersen *et al.* (1996) the He potential curve is always closer to the metal than that for Ne, for both the top and the short-bridge positions with the same incoming atom energy. This is still an open problem.

VII. CHEMISORPTION

A. Atomic chemisorption

We now discuss in some detail atomic chemisorption, though this phenomenon is less important than molecular and dissociative chemisorption as a means to study chemical reactions at surfaces. However, it is possible to extract the main features of chemisorption from this simpler case. We shall focus our attention on three main aspects of this theory: (i) how chemisorption on simple metals can provide an understanding of covalent and ionic adatom-metal bonds; (ii) the problem of lack of charge neutrality within the adatom-metal region where the calculation is performed; (iii) how chemisorption re-

TABLE II. Summary of *ab initio* calculations for several of the chemisorbed systems discussed in the text. For the acronyms defining the theoretical methods see the text. Models in the last column are as follows: EMB, embedding; SC, supercell; SL, slab; CL, cluster; *J*, a jellium substrate, which is ionic and unrelaxed unless labeled by an R (relaxed).

Authors	Systems	Methods	Model
Bagus and Pacchioni (1992)	CO on metals	HF	CL
Bormet *et al.*(1994)	Na, Si, Cl on Al(111)	DFT-LDA	EMB
Feibelman (1991a)	H, S on Rh(001)	DFT-LDA	EMB
Feibelman (1991b)	H_2 on Rh(001)	DFT-LDA	EMB
Feibelman (1992a)	H, and Al on stepped Al	DFT-LDA	EMB
Gravil *et al.* (1996)	O_2 on Ag(110)	DFT-GGA	SC (R)
Gunnarsson *et al.* (1976, 1977)	H on Al	DFT-LSDA	EMB (J)
Hammer *et al.* (1993)	H_2 on Al(110)	DFT-GGA	SC
Hammer *et al.* (1996)	CO on metals	DFT-GGA	SC
Hammer and Nørskov (1995a)	H_2 on metals	DFT-GGA	SC
Hammer *et al.* (1994)	H_2 on Cu(111)	DFT-GGA	SC
Jennison *et al.* (1996)	CO, NH_3 on Pt(111)	DFT-LDA	CL
Kroes *et al.* (1997)	H_2 on Cu(100)	DFT-GGA	SL
Lang and Williams (1978)	H, Li, O, Na, Si, Cl on Al	DFT-LDA	EMB (J)
Stumpf and Scheffler (1996)	Al on Al surfaces	DFT-LDA	SC (R)
Trioni *et al.* (1996)	Si, N on Al	DFT-LDA	EMB (J)
White and Bird (1993)	H_2 on Cu(100)	DFT-LDA	SC
White *et al.* (1994)	H_2 on Cu(100)	DFT-GGA	SC
Wilke and Scheffler (1996a)	H_2 on Pd(100)	DFT-GGA	SC

sults from density-functional–GGA calculations can be interpreted by a simple model based on the Anderson-Grimley-Newns Hamiltonian model.

Note that the theoretical approaches and the adsorption models for the various molecule-metal systems to be discussed in this section are summarized in Table II.

The first studies of adatom chemisorption by the density-functional–LDA method date back to the work of Gunnarsson, Hjelmberg, and Lundqvist (1976, 1977) and Lang and Williams (1975, 1976, 1978). Gunnarsson, Hjelmberg, and Lundqvist (1976, 1977) presented an *ab initio* density-functional–LSDA study of hydrogen chemisorption on a high-density $(r_s=2)sp$ bonded Al-like jellium, including first the periodic structure of the surface by lowest-order perturbation theory with an array of pseudopotentials representing the lattice. Figure 13 shows the binding-energy curves for H on jellium and on Al(100), Al(110), and Al(111) along surface normals with the adatom at different surface positions. The essential part of binding can be explained in the H-jellium model. Here the equilibrium distance $Z_{\rm eq}$ of the atom nucleus from the positive jellium background is 0.6 Å. From the calculation one can see that the induced DOS (Hjelmberg, Gunnarsson, and Lundqvist, 1977) shows a behavior of weak neutral chemisorption with one atomic resonance, which, in terms of the Anderson-Grimley-Newns model, implies that the hopping terms are small. From the induced DOS one can also observe a shift in the broad resonance peak to higher energies with respect to the 1*s* free-atom level. This signals electron transfer from the metal, which is roughly estimated to be 0.1 electrons. In Fig. 14 one can see a charge accumulation to the proton compared to the free-atom situation and the rapid screening of the adatom perturbation inside the metal with the characteristic Friedel oscillations.

A density-functional–LDA calculation of the adsorption properties on the same jellium of several atoms (H, Li, O, Na, Si, Cl) has been performed by Lang and Williams (1975, 1976, 1978). Note that the results of H chemisorption are in agreement with those just discussed by Gunnarsson, Hjelmberg, and Lundqvist (1976, 1977). Figure 15 shows the induced DOS of chemisorbed Cl, Si, and Li at $Z_{\rm eq}$. To explain these results one can apply the concept of the resonant state derived from the Anderson-Grimley-Newns model in the weak-coupling case (see Sec. II.A). Note first that the energy positions of the resonances reflect the relative electronegativities of the adatoms. Observe next that the Li 2*s* resonance level lies above and the Cl 3*p* lies below the Fermi energy, and hence such adatoms are clear examples of positive (Li) and negative (Cl) ionic chemisorption. For Si adsorption there are two valence-electron resonances arising from the 3*s* and 3*p* atomic levels. The partial occupation of the 3*p* resonance, centered on the Fermi level, determines for Si a covalent chemisorption bond. The character of these three different types of bonds is manifested by the charge contour plots in Fig. 16, which are discussed in detail in Lang and Williams (1978).

An important problem tackled in Lang and Williams (1978) is the lack of charge neutrality within the spherical region *I* of radius $R_{\rm sp}$ where self-consistency is achieved, because the perturbation induced by the adatom is not fully screened within *I*. This determines charge disturbances outside *I* which have to be taken into account, at least approximatively, in calculating the adsorption energy $E_{\rm ads}$. Lang and Williams (1978) iden-

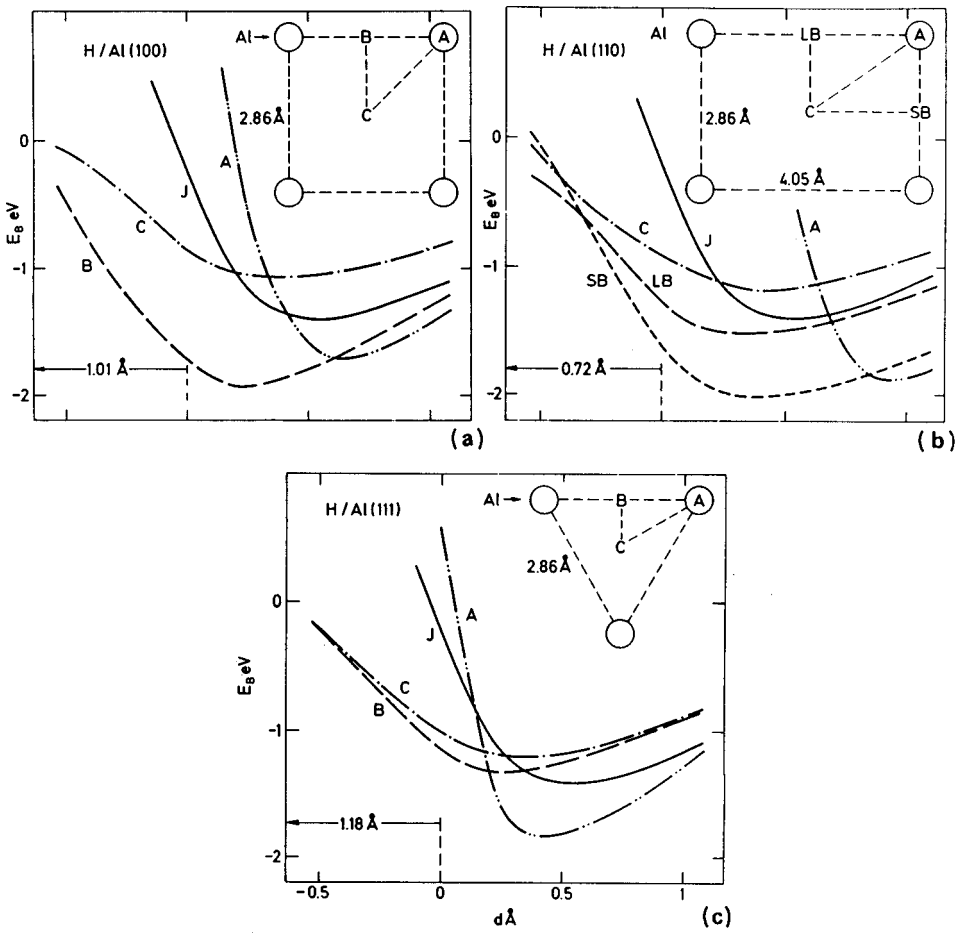

FIG. 13. Calculated binding energy E_B curves for H chemisorbed on semi-infinite jellium (J,r_s=2) and in (A) top, (B, SB, and LB) bridge, and (C) centered positions on the (100), (110), and (111) surfaces of Al, as functions of the H-jellium edge distance d. The distance from the jellium edge to the outermost layer of Al is given in the lower left corner of each panel. From Gunnarsson *et al.* (1977).

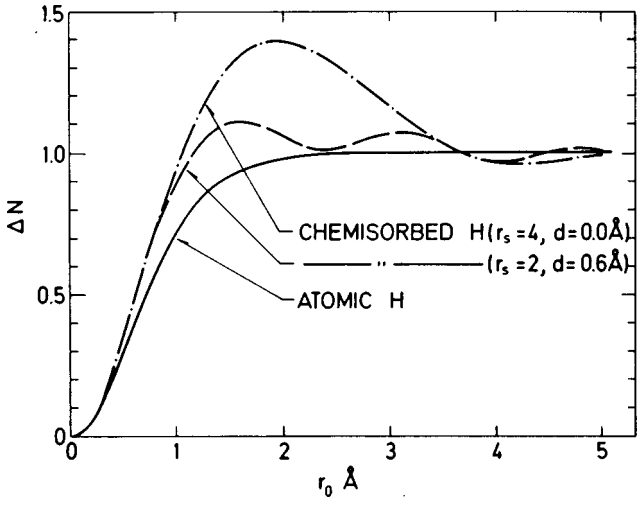

FIG. 14. The electron charge density induced by a H adatom on a semi-infinite jellium at two r_s, compared with the electronic density of atomic H, plotted as the amount of charge within a sphere of radius r_0. The distance d as before. From Gunnarsson *et al.* (1977).

tify two main results of this lack of charge neutrality, Friedel oscillations and a charge distribution outside I. Such contributions are taken into account in the self-consistent loop. In this way, at the end one calculates an amount of electronic charge $Q_{\rm loc}$ within I, due to the presence of the adatom. The leading correction to the

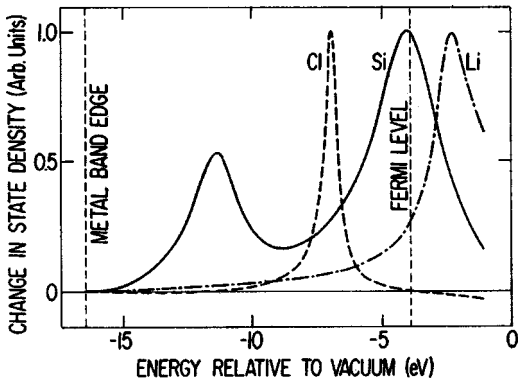

FIG. 15. Induced DOS of Cl, Si, and Li chemisorbed on Al-like jellium at the adatom-surface distance, which minimizes total energy. From Lang and Williams (1976).

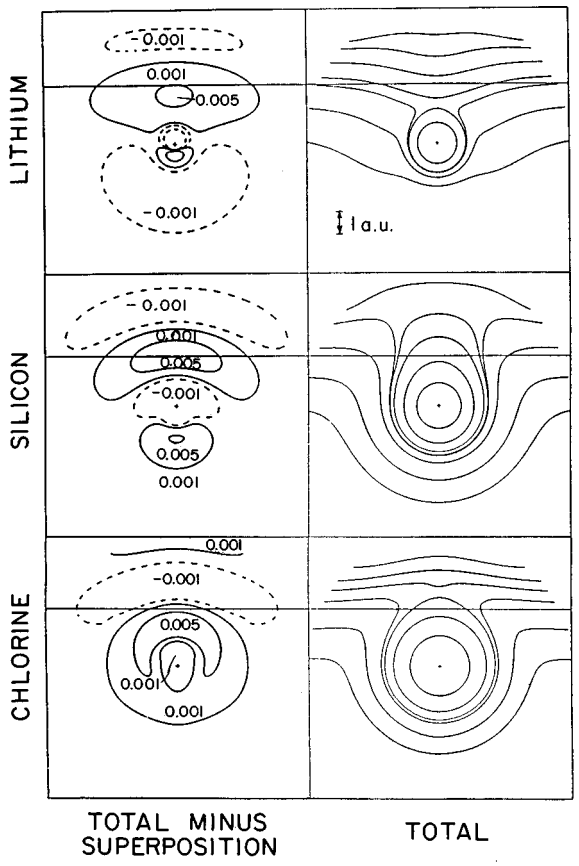

FIG. 16. Electron density contours for chemisorption on a high-density ($r_s=2$) substrate. Upper row: contours of constant electron charge density in a plane normal to the Al-like jellium surface containing the adatom nucleus (+). The solid vertical line is the positive background edge. Lower row: contours of the charge displacements (total minus superposition of atomic and bare-metal electron densities) in electrons/a_0^3. From Lang and Williams (1976).

atomic binding energy (with the vacuum potential being the zero) is

$$\Delta E_{\rm ads} = -\Delta Q_{\rm loc} E_F, \tag{82}$$

where $\Delta Q_{\rm loc}$, defined in Sec. V.B, measures the excess or deficit of electronic charge in I.

The problem of the violation of charge neutrality in a self-consistent calculation of adsorption in a finite region (a sphere with $R_{\rm sp}=7a_0$), embedded in a semi-infinite metal, has been reexamined by Trioni *et al.* (1996). In their work on adatoms on jellium, with $r_s=2.07$, where, unlike the all-electron approach in Lang and Williams (1978), the atoms are treated by pseudopotentials (Bachelet, Hamann, and Schlüter, 1982), these authors have applied the generalized phase-shift method (see Sec. V.B) to obtain systematically the induced DOS in the whole space due to the presence of the adsorbate. Such induced densities of states include changes within the embedding region and the substrate. By this method the excess or deficit of electron charge in the whole system is measured by ΔQ defined in Sec. V.B. We recall that ΔQ is different from $\Delta Q_{\rm loc}$, except in the case of perfect screening, when they are both zero. The adsorption energy is determined using a grand-canonical functional (see Sec. V.B). Figure 17 shows the atom-metal interaction energy for Si on Al-like jellium as a function of the atom-surface distance from Lang and Williams (1978) (solid line) and Trioni *et al.* (1996) (dashed line), respectively. The inset displays ΔQ. If we do not introduce the grand-canonical correction, from the value of ΔQ at $Z_{\rm eq}$ in Fig. 17, and from Eq. (73), we can see that $E_{\rm ads}$ is lowered by about 0.28 eV. Note that $\Delta Q = 0.072$ electrons, while $\Delta Q_{\rm loc}=0.09$ electrons. No estimate of $\Delta Q_{\rm loc}$ is reported in Lang and Williams (1978) for comparison. The lack of charge neutrality determines a more significant correction to $E_{\rm ads}$ for a more ionic chemisorption bond such as N on Al-like jellium. In this case the correction amounts to a negative shift of about 0.7 eV (Trioni *et al.*, 1996).

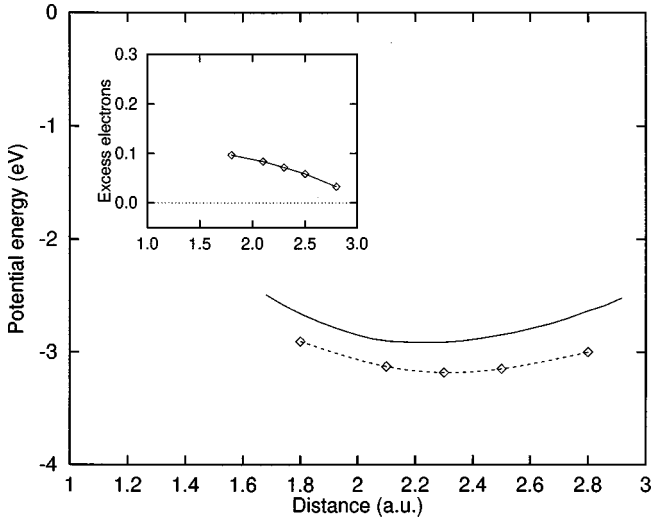

FIG. 17. Adatom-metal potential energies of Si on Al-like jellium, as functions of the atom-surface distance: solid line, from Lang and Williams (1978); broken line, from Trioni *et al.* (1996). The inset gives ΔQ, as a function of the atom-surface distance.

A density-functional–LDA calculation of adatoms on Al(111) considering the lattice structure of the substrate has been performed by Bormet, Neugebauer, and Scheffler (1994). These authors point out that Al is not a free-electron metal, since: (i) the top layer of Al(111) relaxes slightly inward, not outward as for a free-electron metal; (ii) the jellium model gives a negative surface energy for Al, so, it is important to have results that take into account the atomistic structure of the metal and its electronic energy band shapes in an *ab initio* calculation of adsorption on Al. Figure 18 shows the induced DOS for single adatoms of Cl (dotted line), Si (dot-dashed line), Na (dashed line), and the DOS for clean Al (solid line). There is excellent agreement for Cl and Na with the induced DOS calculated by Lang and Williams (1978) on jellium. The biggest differences are found for the Si-3p induced resonance, where the atomistic substrate splits it into occupied bonding and empty antibonding states. Additional insight into this covalent chemisorption bond can be found from the charge displacements of the system presented by Bormet, Neugebauer, and

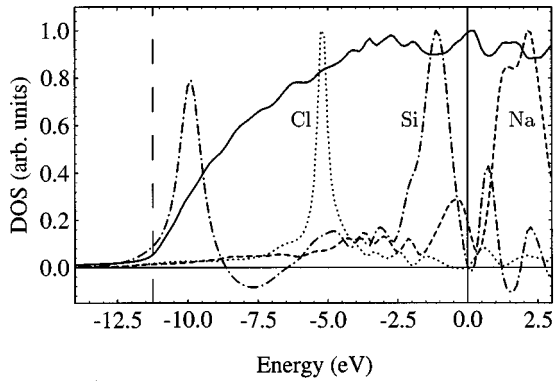

FIG. 18. Induced densities of states: dashed line, Na; dot-dashed line, Si; and dotted line, Cl on Al(111). The solid line gives the local DOS of the Al substrate. The solid vertical line is the Fermi level. From Bormet *et al.* (1994).

Scheffler (1994). The adsorption energy for Si on Al(111) is calculated with the grand-canonical functional. But note that $\Delta Q_{\rm loc}$, not ΔQ, is considered in the adsorption energy expression. In practice, this discrepancy is not so important, as Bormet, Neugebauer, and Scheffler (1994) report a value of $\Delta Q_{\rm loc}=0.01$ electrons, giving a negligible contribution to $E_{\rm ads}$. However, $E_{\rm ads}$ in Bormet, Neugebauer, and Scheffler (1994) is more than 1 eV higher than in Lang and Williams (1978) and Trioni *et al.* (1996). Here the question arises whether, in an Al substrate with a lattice structure, the adatom perturbation is essentially localized in the embedding region or whether it might be an artifact due to the choice of the localized basis set selected for the numerical solution. We recall that an expansion in a plane-wave basis set is used in Trioni *et al.* (1996). In conclusion, the results in Bormet, Neugebauer, and Scheffler (1994) give support to those for adatoms on a jellium substrate, though important differences are present. Such results are also complemented by calculations for periodic adlayers within a supercell framework, with very good agreement.

Ab initio calculations of H and S adatoms on a transition-metal surface, i.e., Rh(001), have been performed by Feibelman (1991a). The adatom binds in a fourfold hollow. The H adatom lies rather close to the outer Rh layer, and it is better screened than the S adatom, which is larger and lies higher above the surface. In fact, $\Delta Q_{\rm loc}=7\times10^{-4}$ electrons for H and $\Delta Q_{\rm loc}=4\times10^{-3}$ electrons for S, both determining a smaller violation of the local charge neutrality than for that for adatoms on Al. This trend is to be expected owing to the more localized character of transition-metal electrons.

A systematic study of atomic, dissociative, and molecular chemisorption on several metals has been made by Hammer and Nørskov (1995a, 1995b, and 1997). The aim of such research is not only to perform extensive *ab initio* calculations, but also to compare their results with those worked out by a model, which can explain the main trends of bonding on metal substrates with partially filled (say f their fractional filling) or full d bands. Again their model is based on the Anderson-Grimsley-

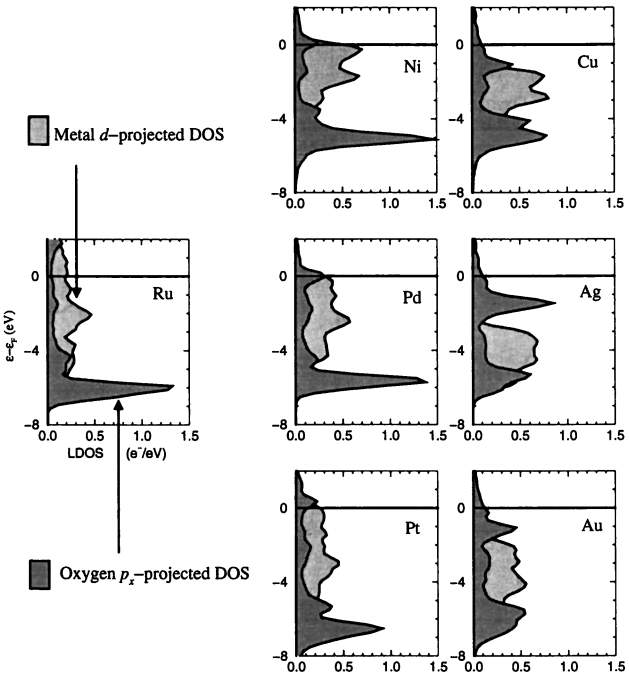

FIG. 19. Projected DOS into the oxygen p_x state (dark shaded area) for an adatom 1.3 Å above the close-packed surfaces of late transition and noble metals. The light shaded area gives the metal d-projected DOS for the respective metal surfaces. From Hammer and Nørskov (1977).

Newns Hamiltonian. They assume that the bond formation occurs in two steps. First the relevant adatom orbital or orbitals interact with the sp band, which is fairly wide. This broadens the adatom orbital, forming a single resonance in agreement with the weak-coupling case of the model. Next they consider the coupling of this resonance to the d bands of the substrate. Since the characteristic width W of the d bands is smaller than the hopping terms V, following the strong-coupling case of the model, this causes the splitting of the above resonance into a bonding and an antibonding state, one below and one above the metal d bands. This result is shown in Fig. 19, where the *ab initio* LDOS projected onto an oxygen adatom p_x state and the surface DOS of the sheer d bands are plotted for various metals. In a one-electron picture, with just one adatom orbital of energy E_A and one d band centered at energy E_d, the d-band contribution $E_{d-\rm hyb}$ to the total adsorption energy $E_{\rm ads}$ can be written down using perturbative arguments similar to those used to obtain the first term on the right in Eq. (79):

$$E_{\rm ads}=E_0+E_{d-\rm hyb} \tag{83}$$

$$E_{d-\rm hyb}=-(1-f)(W_d-\Delta_d)-2(1+f)VS. \tag{84}$$

In Eqs. (83) and (84) E_0 is the sp contribution to the bonding energy, which is the largest absolute energy, but cannot account for the different values of $E_{\rm ads}$ on different metals; $W_d=\sqrt{4V^2+\Delta_d^2}$, $\Delta_d=E_d-E_A$, and S is the overlap between the adsorbate state and the metal d states. The first term multiplied by $(1-f)$ is an attractive one, unless the d band is completely full, and is due to

the hybridization between the adatom orbital and the *d*-metal states. The second term represents the Pauli repulsion energy. The crucial term is the coupling $V<0$. This depends on the adatom position and for a fixed adsorbate geometry is only a property of the metal substrate. A comparison between the model adsorption energy and that calculated by the density-functional–GGA within the supercell method for O on various metals is presented in Fig. 20. One observes that this model accounts for the *ab initio* results very well. Note also that Au has got the most energy extended *d*-band states, the largest hopping terms, and hence the largest repulsion (Hammer and Nørskov, 1997).

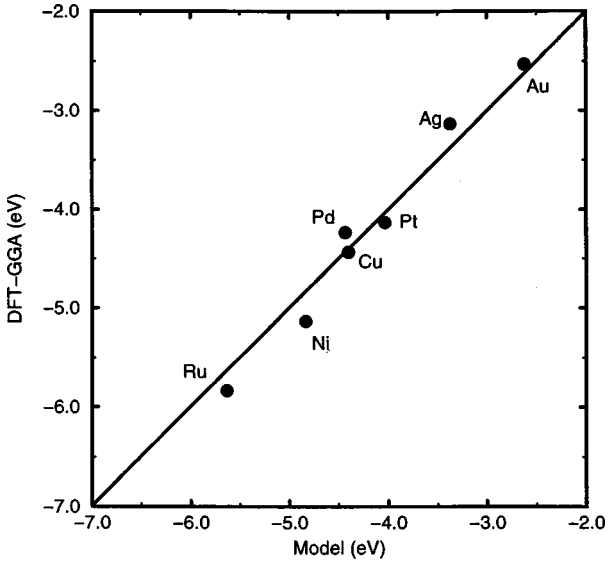

FIG. 20. The density-functional–GGA oxygen chemisorption energies vs the Anderson-Grimley-Newns model energies for various noble and transition metals. From Hammer and Nørskov (1977).

B. Dissociative chemisorption

One of the fundamental problems in the gas-surface interaction is the study of dissociative chemisorption, whose dynamical counterpart is called the dissociative sticking problem. In fact, dissociative chemisorption is not only the prototype of one of the simplest chemical reactions at surfaces, the simplest being atomic sticking, but is also an example of the importance of molecule-surface adiabatic properties for the dynamics. In this article we shall concentrate mainly on recent work in which the statics of dissociative adsorption are computed within an *ab initio* framework. The reader is directed to Darling and Holloway (1995) for a review on this problem, where phenomenological models are also discussed.

We shall deal mostly with dissociative sticking of H_2 on metals. This process is assumed to occur as a quantum collision event on the adiabatic ground-state molecule-metal potential-energy surface (PES). Here the surface provides an energetically more convenient setup for the two dissociated H adatoms. Of course substrate excitations, especially electron-hole pairs (Brivio and Grimley, 1983; Brivio, 1987), may be important to assist sticking, but they are at present ignored in all calculations, where the potential-energy surfaces are taken as the adiabatic manifold on which one develops the dynamical calculation of the sticking probability (coefficient) *s*. We shall focus our attention mainly on two outstanding results of recent *ab initio* calculations, the presence or absence of an activation barrier and the multidimensional character of the PES.

Following previous work on H on Rh(001) (Feibelman, 1991a), the first paper that aims at an *ab initio* calculation of adiabatic electronic properties of a molecule on a metal is by Feibelman (1991b), who considers the orientation dependence of the binding energy of a H_2 molecule (with its axis parallel to the surface) a few a_0's above the Rh(001) surface. The main result of this 3D calculation is the multidimensional character of the dissociating PES compared to the simplified 1D one proposed in the textbooks (see Zangwill, 1988). Other interesting points are that

(i) The H-metal bond begins to form at the rather unsymmetric bridge-to-bridge orientation. This configuration is energetically favored with respect to more symmetric ones (top-to-top and hollow-to-hollow), even if the equilibrium position of the H adatoms are the four-fold hollows.

(ii) The bridge-to-bridge orientation maximizes the H atoms' coordination with metal atoms; three Rh atoms are involved, as displayed in Fig. 21(c), which should be compared with the molecular orientations in Figs. 21(a) and 21(b).

Since extensive experimental measurements of *s* (Anger, Winkler, and Rendulic, 1989; Michelsen and Auerbach, 1991; Rettner, Auerbach, and Michelsen, 1992; Rettner, Michelsen, and Auerbach, 1995) have been performed on H_2 on Cu, a great deal of theoretical work has been devoted to such systems. Such work includes *ab initio* calculations of the PES and numerical solutions of the time-dependent Schrödinger equation. To determine *s*, the first work made use of PES guesses (Darling and Holloway, 1995), while the most recent studies begin their quantum simulations from the above-mentioned PES calculated from first principles.

A first, *ab initio* calculation of the PES for H_2/Cu(111), with the H_2 molecule parallel to the surface and dissociating in the optimum configuration with the axis perpendicular to the Cu-Cu bridge position (bridge-to-hollow), over which it is centered, is displayed in Fig. 22 (Hammer *et al.*, 1994). Such a PES is a function of two coordinates, the interatomic distance *b* and the molecule-surface distance *Z*. The PES in the lower panel, calculated within a density-functional–GGA framework, shows an activation barrier to dissociation $E_{act}=0.73$ eV, when the bond length has been extended more than 33%. This barrier is found in the exit channel. Convergence studies, mainly by increasing the number of **k** points in the supercell and the number of electronic states, give instead a barrier with 0.48 eV $\leqslant E_{act} \leqslant 0.54$ eV, in better agreement with the experi-

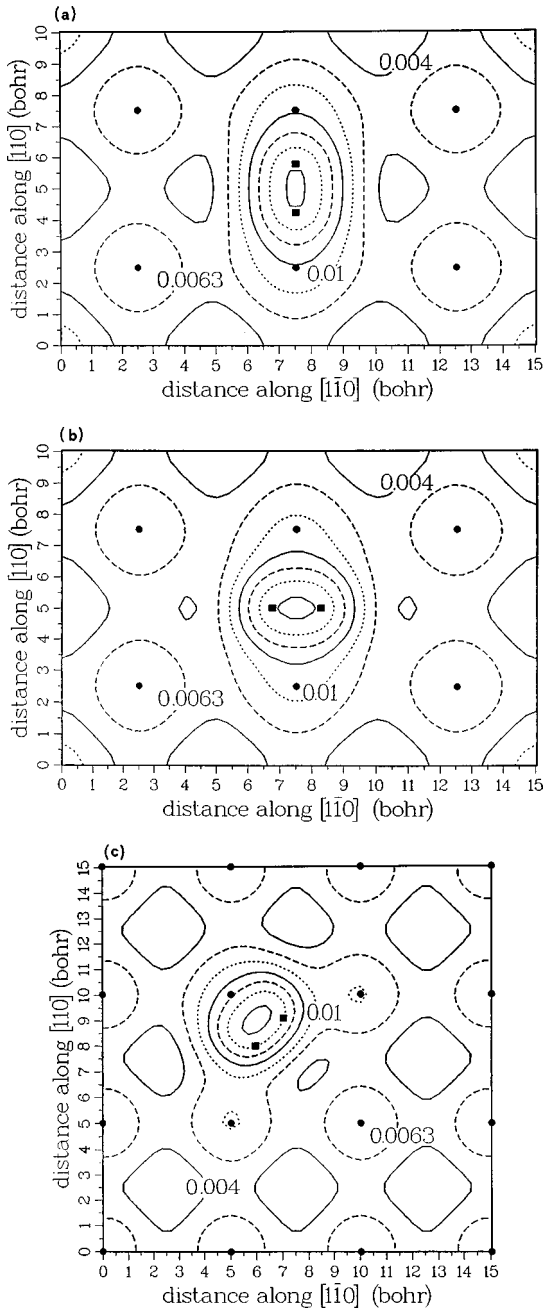

FIG. 21. Charge contour plots in electrons/a_0^3 in a plane $2.98a_0$ above the outer Rh nuclei (heavy dots) for three different H_2/Rh(001) orientations with the H nuclei at $3.98a_0$ (heavy squares). Every fifth contour represents a change in charge density of a factor of 10. (a) A hollow-to-hollow molecular orientation; (b) top-to-top bonding, and (c) bridge-to-bridge case. From Feibelman (1991b).

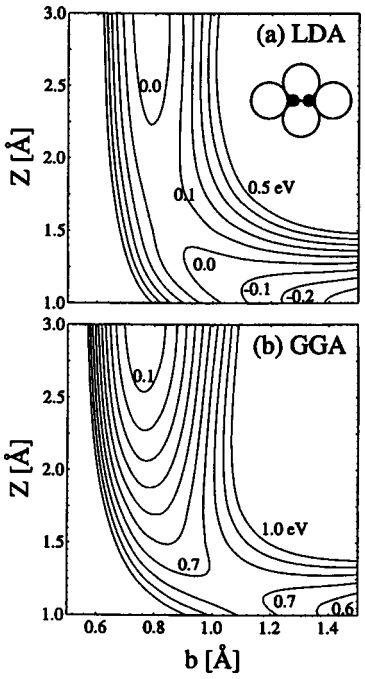

FIG. 22. The potential-energy surface for H_2 dissociation over Cu(111): (a) calculated within the density-functional–LDA model and (b) calculated within the density-functional/generalized gradient approximation. The inset shows the geometry. b and Z are the interatomic and molecule-surface distances, respectively. From Hammer *et al.* (1994).

mental findings (Hammer *et al.*, 1994). The comparison between E_{act} calculated within the GGA and LDA frameworks is an extremely useful example, pinpointing the failure of the latter approximation for E_{act}. Observe the upper panel in Fig. 22, where the potential-energy surfaces are computed by the LDA. The two main discrepancies between the LDA and GGA results are an extremely low activation barrier and a shift in the entrance channel. A significantly larger activation barrier by the GGA is also found for H_2/Cu(100) (White *et al.*, 1994). An explanation for the inability of the LDA to treat chemisorption activation barriers was first proposed for H_2/Al(110), already investigated by Hammer *et al.* (1992), by Hammer, Jacobsen, and Nørskov (1993). These authors made use of the Harris and Liebsch (see Sec. VI) approach in order to account for a nonlocal exchange-correlation effect. Recall that in the study of a He atom close to a metal surface, after introducing a perturbation expansion in the adsorbate pseudopotential, Harris and Liebsch point out two competing effects. The first effect is the removal of electronic charge in the outer region of the adatom, because the metal Bloch waves orthogonalize to the adatom ones (orthogonalization contribution). This term turns out to be an energy cost due to the Pauli repulsion between the adatom and the metal electronic wave functions. The second contribution is an attractive one, due to the potential gain of the metal states in the presence of the adatom (hybridization contribution). For H_2/Al(110) the orthogonalization contribution is greatest at molecule-metal distances just beyond that of dissociation, creating an exchange-correlation hole around the molecule which is made deeper by the GGA than by the LDA. A larger orthogonalization energy and a more repulsive activation barrier follow. For a more complex metal surface with d bands there may or may not be an activation barrier for H_2. For a closer look at this feature, see Hammer and Nørskov, 1995a, 1995b, 1997; Kratzer, Hammer, and Nørskov, 1996. One follows a two-step approach similar to treatment of atomic chemisorption

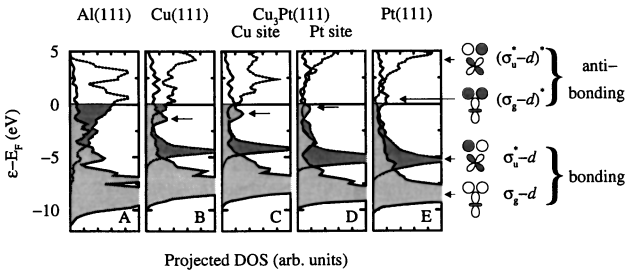

FIG. 23. The projected metal-σ_g (light shading) and σ_u^* (dark shading) DOS of H_2 on Al(111), Cu(111), $Cu_3Pt(111)$, and Pt(111), with an H-H separation of 1.2 Å and a height from the surface of 1.5 Å. The nature of the wave function at different peaks in the DOS is depicted by the schematics at the right of the figure. From Hammer and Nørskov (1995a).

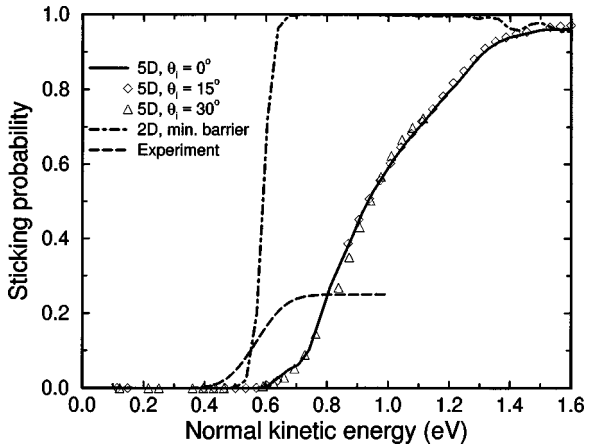

FIG. 24. Sticking coefficient vs normal kinetic energy for H_2 molecules, initially in the vibrational and rotational ground state, on Cu(111). θ_i is the molecule-surface polar angle. Solid line, 5D calculations; the dot-dashed line, 2D calculations; dashed line, the experimental results. From Gross (1996).

within the Anderson-Grimley-Newns model framework. First the interaction of the H_2 bonding σ_g and antibonding σ_u^* states with the *sp* electrons is shown to broaden such molecular states. Then the interaction of such resonances with the narrow metal *d* bands determines two bonding states, σ_g-d, σ_u^*-d and two antibonding states $(\sigma_g-d)^*$, $(\sigma_u^*-d)^*$. The σ_u^*-metal interaction is always attractive, being its antibonding state above the Fermi level. On the other hand, the interaction with the σ_g state changes with the substrate. For Cu its antibonding state is below the Fermi level and when filled it causes a repulsive interaction, so that the net result of the two contributions is a repulsive barrier. For other metals, such as Pt, this resonance is shifted above the Fermi level, so that the σ_g-d interaction changes sign and there is a negative barrier (see Fig. 23). Discussions of the reactivity of the H_2-metal and of the H_2-metal alloy surface from *ab initio* results can also be found in Wilke, Cohen, and Scheffler (1996) and Hammer and Scheffler (1995).

Once the *ab initio* potential-energy surfaces are obtained, one can work out *s* by quantum-dynamic calculations. We shall present results only for *s* in which the H_2 molecule is initially in the vibrational ground state. Figure 24 shows *s* as a function of the impinging H_2 molecule's translational kinetic energy normal to the Cu(111) surface, $E_{\rm kin}$, for various polar angles of incidence θ_i (Gross, 1996). This work is based on PES calculations of Hammer *et al.* (1994) which give too high an activation barrier. In Fig. 24 the dot-dashed curve reports a 2D calculation for a flat surface corresponding, as already outlined, to the minimum activation barrier in Fig. 22, while the dashed line shows the experimental results (Rettner, Michelsen, and Auerbach, 1995). The solid line describes *s* from a 5D quantum simulation which, beyond *b* and *Z*, includes the two surface coordinates $\mathbf{R}_\parallel$ and an average over twelve azimuthal orientations φ (Gross *et al.*, 1994). All curves qualitatively display the characteristic behavior of activated sticking. At first, for very small $E_{\rm kin}$, *s* is very low due only to tunneling through the activation barrier; then, as $E_{\rm kin}$ increases, so does *s*, reaching saturation for larger $E_{\rm kin}$. Looking at the 5D simulation result, one notes that for $E_{\rm kin}\geqslant 0.6$ eV (at about 0.15 eV below the minimum activation barrier), an increase in *s* becomes classically possible, due to a softening of the H_2 bond at the surface. Comparison between the 2D and the more realistic 5D calculations of *s* shows that the two are very different. The higher-dimension result, which takes into account a distribution of barrier heights in the unit cell, and hence the lateral corrugation of the surface, varies from the optimum barrier at $E_{\rm act}=0.73$ eV to $E_{\rm act}=1.43$ eV. Similar results are also found for the $H_2/Cu(100)$ system, where the lowest barrier occurs for dissociation into neighboring bridge and hollow sites (White and Bird, 1993; White *et al.*, 1994). Going back to Fig. 24, we observe that, apart from a shift in *s* towards lower $E_{\rm kin}$ for more accurate values of $E_{\rm act}$ (see above), the calculated 5D and the experimental *s* show the same onset of sticking. However, for larger $E_{\rm kin}$ the theoretical *s* saturates differently from the experimental. The high-dimensionality effect for H_2 sticking is stressed in Fig. 25, where *s*, as a function of $E_{\rm kin}$, from a full 6D quantum simulation using an *ab initio* PES, is compared to that obtained from a lower-dimension PES for $H_2/Cu(100)$ (Kroes, Baerends, and Mowrey, 1997). These results confirm that all molecular degrees of freedom have to be included in the simulation of *s*, in particular, the two rotational ones φ and θ_i, the polar degree of freedom depending on the angle formed by the molecular axis with respect to the surface not considered in Gross *et al.* (1994). The same conclusions are drawn by Dai and Light (1997) from a 6D quantum simulation of *s* for $H_2/Cu(111)$ starting from a PES calculated by the London, Eyring, Polanyi, and Sato method (Sato, 1955), constructed incorporating the *ab initio* information in Hammer *et al.* (1994).

A different dependence of *s* on $E_{\rm kin}$ occurs for a system such as $H_2/Pd(100)$ (Rendulic, Anger, and Winkler, 1989), for which first-principles calculations have proven that there are activated and nonactivated paths for dissociation (Gross, Wilke, and Scheffler, 1995;

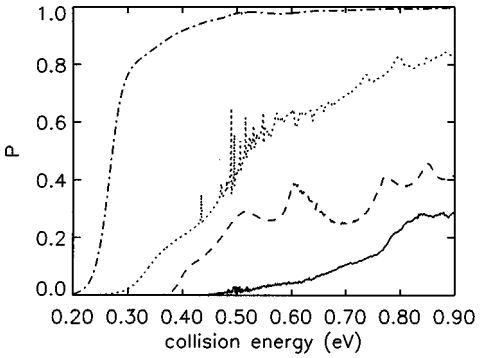

FIG. 25. Sticking coefficient vs normal kinetic energy for H_2 molecules, initially in the vibrational and rotational ground states, on Cu(100): solid line, 6D calculations; dot-dashed line, 2D calculations; dotted line, 4D calculations including parallel translational motion; dashed line, 4D calculations including rotational motion. From Kroes *et al.* (1997).

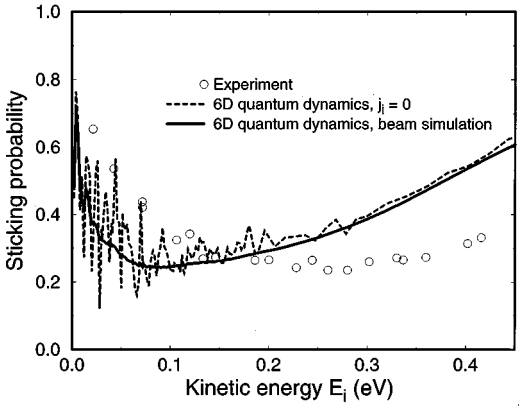

FIG. 26. Sticking coefficient vs normal kinetic energy for a H_2 beam under normal incidence on a Pd(100) surface: dashed line, calculations of molecules initially in the rotational ground state ($j_i=0$); solid line, H_2 molecules with an initial rotational and energy distribution adequate for molecular beam experiments; empty circles refer to experiment. From Gross *et al.* (1995).

Wilke and Scheffler, 1996a). This could explain why for this system s decreases when $E_{\rm kin}$ is increased, without invoking the existence of a molecular precursor state. Figure 26 displays both the experimental s and that obtained from a 6D quantum simulation based on an *ab initio* PES.

In conclusion, we wish to point out that the multidimensional character of H_2 sticking on metals causes a wealth of effects. These include the normal energy scaling of s, regardless of strong surface corrugation, as a compensating result due to the so-called energetic and geometric corrugations (Darling and Holloway, 1994), steering mechanisms (Kay *et al.*, 1995; Wilke and Scheffler, 1996a), enhancement of sticking due to intramolecular vibrational excitations, and the relevance of rotations of the incoming molecule (Dai and Light, 1997). Usually rotations suppress sticking, though this phenomenon is more important for the so-called cartwheel rotations (with the rotational axis preferentially parallel to the surface) than for helicopter rotations (with the rotational axis preferentially perpendicular to the surface) (Gross, 1996). In this second case and for a system with an activation barrier in the exit channel, such as H_2/Cu(111), helicopter rotations seem to favor sticking (Darling and Holloway, 1995; Dai and Light, 1997).

First-principles calculations for the adsorption of O_2 on Ag(110) are worked out by Gravil *et al.* (1996). This is a complex system, which displays three wells, a physisorption well, a molecular well, and a dissociative chemisorption well. Gravil *et al.* (1996) concentrate on the peroxolike molecular chemisorbed state. However, their calculations are not conclusive, as the minimum pathway into the chemisorbed four-hollow state shows no barrier from the gas phase, in contrast to experiments that show an activated chemisorption process, implying the existence of a barrier. This result underscores the present difficulty of a first-principles calculation of dissociative chemisorption for a more complex system than H_2 on metals.

C. Molecular chemisorption

Molecular chemisorption is currently the subject of several *ab initio* studies, both experimental (Batteas *et al.*, 1996; Nilsson *et al.*, 1997) and theoretical (Hu *et al.*, 1994; Lewis and Rappe, 1996; Fahmi and van Santen, 1997; Majumdar and Balasubramanian, 1997; Pacchioni *et al.*, 1997; Yang and Whitten, 1997). A review of such results is beyond the scope of this article. However, we believe it to be instructive to discuss two efforts, related to CO chemisorption on metals having a d band, for which results have just been worked out within two different *ab initio* frameworks, namely, (i) an attempt to predict the chemical activity of surfaces on the basis of surface electronic properties alone; (ii) an estimate of the lateral interaction between two adsorbed molecules, which is an example of the present frontier computational effort in surface science.

Experimental and theoretical studies suggest that an electron donation from the CO 5σ filled orbital to the metal sp and d bands and a backdonation from these metal bands to the CO doubly degenerate empty $2\pi^*$ orbital mainly account for this chemisorption bond (Bagus and Pacchioni, 1992). According to the model already introduced for atomic and dissociative chemisorption (Hammer, Morikawa, and Nørskov, 1996; Hammer and Nørskov, 1997), one can explain the *ab initio* results for CO adsorption by again splitting the bonding into two steps: first the interaction of CO with the metal sp bands broadens and shifts the 5σ and $2\pi^*$ orbitals down; second the interaction of these resonances with the d-metal states determines, as before, two bonding and two antibonding states (see Fig. 27). Hence the d contribution to the adsorption energy $E_{d-\rm hyb}$ can be written in the form of a hybridization gain and an orthogonalization energy cost, for the 5σ and the $2\pi^*$ orbitals, respectively, via a simple formula:

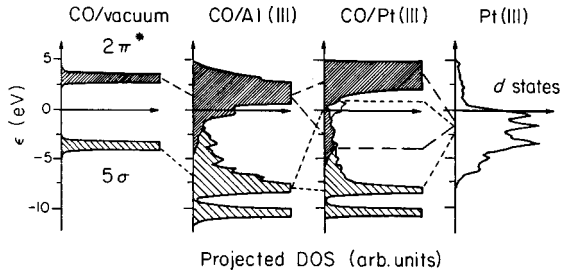

FIG. 27. Densities of states projected onto the 5σ and 2π orbitals of CO. From left: the CO molecule 5σ and $2\pi^*$ orbitals, the CO/Al(111) and CO/Pt(111) projected DOS onto the 5σ and $2\pi^*$ orbitals, and the metal d-projected DOS. From Hammer *et al.* (1996).

$$E_{d-\mathrm{hyb}} = -4\left[f\frac{V_\pi^2}{E_{2\pi}-E_d} + fS_\pi V_\pi\right] - 2\left[(1-f)\frac{V_\sigma^2}{E_d-E_{5\sigma}} + (1+f)S_\sigma V_\sigma\right], \quad (85)$$

where E_d is the center of the d band, while $E_{5\sigma}$ and $E_{2\pi}$ are the energies of the sp renormalized adsorbate states. The overlap terms, S_π and S_σ, and the coupling terms, V_π and V_σ, are defined in analogy with those in Eq. (84). From an examination of Fig. 28, which refers to several CO-metal systems, one observes a linear relationship, with a slope very close to one, between $E_{d-\mathrm{hyb}}$ and the chemisorption energy of CO, calculated in a density-functional–GGA framework by using a supercell with a quarter monolayer of adsorbed CO at the top position. One also deduces that the contribution of the sp bands to E_{ads} amounts to about -0.5 eV.

In the case of CO adsorption on metallic overlayers, x-ray photoelectron spectroscopy (Rodriguez and Goodman, 1992) demonstrates a correlation between core-level energy shifts of the metal film atoms, measured before adsorbing CO, and CO desorption temperatures. It has been suggested that such a change in the core-level energies reflects the variation of the surface d band upon formation of the metal overlayer (Hennig, Ganduglia-Pirovano, and Scheffler, 1996). For this reason Hammer, Morikawa, and Nørskov (1996) identify such a shift in the center of the d band with a downward shift in the surface core level. Assuming that the hybridization term with the $2\pi^*$ orbital dominates Eq. (85), Hammer, Morikawa, and Nørskov (1996) establish a linear relationship between the differential change in $E_{d-\mathrm{hyb}}$ and the change in the position of the d-band center, namely,

$$\delta E_{d-\mathrm{hyb}} \simeq \left[-4f\frac{V_\pi^2}{(E_{2\pi}-E_d)^2}\right]\delta E_d . \quad (86)$$

If the CO chemisorption energy shift $\delta E_{d-\mathrm{hyb}}$ is proportional to the negative peak shift of the temperature-programmed desorption, a linear relationship between the renormalized temperature-programmed desorption and the above-mentioned core-level shifts should occur.

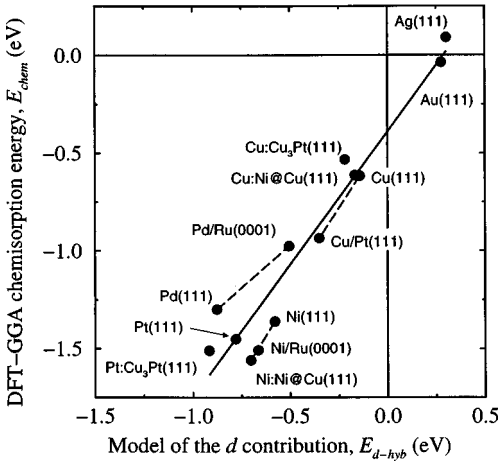

FIG. 28. Comparison between the model and the full density-functional–GGA chemisorption energies for CO on a number of metal systems. From Hammer *et al.* (1996).

Such a relationship is demonstrated by Hammer, Morikawa, and Nørskov (1996). In conclusion, this result is a promising effort, though to be taken with some care (Ganduglia-Pirovano, Kudrnovský, and Scheffler, 1997), in attempting to obtain trends for the catalytic activity of different surfaces from the adiabatic electronic properties.

Several theoretical investigations have been devoted to calculating the interaction between adsorbate particles. For a review including phenomenological models see Einstein (1995). To define the lateral interaction energy, we recall first that in any *ab initio* calculation of adsorption we can only access the total energies of the system under investigation. This is true as well as for an isolated adsorbate. For this reason the lateral interaction energy E_{lat} can be introduced as the difference between total energies, as we explain below. If we deal with an isolated pair of adsorbates, the operative definition of E_{lat} can be expressed as

$$E_{\mathrm{lat}} = E_{\mathrm{ads}}^{1+2} - E_{\mathrm{ads}}^{1} - E_{\mathrm{ads}}^{2} + E_{\mathrm{surf}}, \quad (87)$$

where E_{ads}^{1+2} is the total energy of the adsorbates plus the metal, $E_{\mathrm{ads}}^{1/2}$ is the total energy of either one or two adsorbates plus the metal and E_{surf} the bare semi-infinite metal energy. To our knowledge such a calculation has not yet been performed for two isolated adsorbed molecules on a realistic substrate from first principles. However, if one takes into account an array (even a very dilute one) of molecules, preliminary results exist in work that takes advantage of present-day capability for parallel computing (Jennison *et al.*, 1996). In this case Jennison *et al.* (1996) consider an overlayer of seven molecules with one at the center of the surface on a cluster of Pt atoms. Here the pair lateral interaction E_{lat} is estimated by total-energy differences divided by the number of pairs. The change of E_{lat} with the coverage indicates that the pair interaction is not sufficient to ex-

plain lateral interactions in CO, and many-body interactions may be needed when more than two adsorbates are considered.

D. Other topics

The recent advances in computational tools have allowed for extensive *ab initio* investigations of other aspects of chemisorption particularly important for perspective applications. We shall only very briefly mention a couple of them, in which isolated adsorbates are considered, namely, studies of coadsorption and adatom diffusion.

In the theoretical treatment of coadsorption, Wilke and Scheffler (1995, 1996b) discuss the poisoning activity of Pd(100) by a sulfur adlayer and the drastic reduction of the sticking coefficient of H_2. As already pointed out, at a free Pd(100) surface, H_2 dissociates spontaneously, but S adsorption builds up energy barriers so that the sticking coefficient for S coverage of $\theta_S = 0.25$ is about three orders of magnitude smaller than that for the free surface. In particular, for H_2 impinging at two hollow sites of Pd(100) (2×2)S there are energy barriers of 0.1 and 0.6 eV at the lowest energy dissociation pathways. Note also that the barriers are in the entrance channel, so that the vibrational energy of the H_2 molecule cannot be used to overcome them. An electronic investigation in terms of the LDOS shows that in the channel with the higher barrier there exists a direct repulsion between the H_2 σ_g state and the spatially localized S–Pd bonding band at -4.8 eV.

In materials growth the understanding of self-diffusion of adatoms is very important. For this reason *ab initio* studies of adiabatic (diffusing) atom-metal properties have been performed in order to obtain information on diffusion barriers and paths. Following an earlier study of a Pt adatom diffusing on Pt(001) (Kellogg and Feibelman, 1990), Feibelman (1990) explains the diffusion of an Al adatom on Al(001) along the $\langle 100\rangle$ or $\langle 010\rangle$ direction by an exchange mechanism which involves a surface atom. In fact, for this mechanism the diffusion barrier energy is less than 1/3 that for adatom hopping, though the exchange energy is shown to depend somewhat on the number of slabs used by Feibelman (1990) in the calculation (Stumpf and Scheffler, 1996). The importance of surface steps in adatom diffusion has also been analyzed in detail. Again Feibelman (1992a) demonstrates that an H adatom on a stepped Al(331) surface prefers to be located at step edges, while an Al adatom is more attracted to step bottoms. Hence Al migration occurs along terraces and H migration along steps. For recent extensive calculations of the self-diffusion of an Al adatom on various (stepped) Al surfaces see Stumpf and Scheffler (1996).

VIII. CONCLUSIONS

In this review we have tried to describe the theoretical approaches developed mostly in the last two decades to deal with the adiabatic properties of the molecule-metal interaction. We observe that the greatest progress in this field in the 1990's has been due to the exceptional improvement in computational facilities. With massively parallel processors able to handle up to Gflop:s for each processor it is now possible to perform *ab initio* calculations in regions containing one to two hundred atoms depending on the system under investigation.

But systematic studies of few-molecule/metal systems in order to critically compare, for example, adsorption energies worked out with the embedding, the cluster, the slab, and the supercell approaches by using both HF and density-functional methods, do not at present exist. The various interests and backgrounds of the scientists involved in this field, as well as the complexity and the numerical difficulties of dealing simultaneously with very different methods, have been responsible for this situation. Methods that require more delicate mathematical tools, such as the Green's-function embedding treatment, are now used less often than other, conceptually simpler, approaches such as the slab/supercell and cluster methods (Bird and Gravil, 1997). In fact those latter approaches have provided an easier route for computing total energies and practically all chemisorption energetics obtained in the last few years, as outlined in Sec. VII. There are, however, two points in favor of the Green's-function embedding approach. First, this method requires fewer atoms in the self-consistent calculations than the slab/supercell method for a good convergence of the physical properties of the system; second, since it takes into account a continuum of electronic states due to a semi-infinite substrate, it is more suitable for describing spectroscopic properties such as LEED, photoemission, and Auger spectrum intensities (Ishida, 1997). The question of which approach, either the slab/supercell or the cluster approach, is better is still open. A contribution to this discussion by Bird *et al.* which summarizes the main feelings of theoreticians working in this field follows:

> In the limit of a very large number of atoms such methods must converge to the same answer, but the rate of convergence need not be the same. Our own feeling is that supercell calculations converge faster, and so for limited system sizes provide a better approximation to the ideal case. To date computational resources have not allowed a sufficiently detailed comparison to take place, because it is very expensive to increase the system size in either method to full convergence (Bird, White, and Gravil, 1996).

We believe that this problem will be fully settled in the next few years.

Areas still open for development in the theory of adiabatic molecule–metal interactions include the following:

(i) For a noble gas-metal system, the search for a nonlocal density functional to treat accurately the energy at *all* gas-metal distances, so as to provide a seamless treatment of the repulsion and of the van der Waals attraction. Eventually one should like to be able to do the same for reactive adsorbates, e.g., in dissociative chemi-

sorption, where critical features of the PES may occur when one or more bonds are near their dissociation limit.

(ii) The study of electronically excited PES. For metal substrates, the PES continuum due to the creation of delocalized electron-hole pairs is well understood (Brivio and Grimley, 1983). But the localized excitations of isolated adsorbates may, in specific cases, persist into the region where the bonds in the adsorbate are breaking and new bonds to the substrate are being formed. This is important for the dynamics and could significantly affect the calculated dissociative sticking coefficients.

(iii) The *ab initio* investigation of a heterogeneous catalytic reaction by coupling a density-functional calculation (Stampfl and Scheffler, 1997) with a multidimensional solution of the time-dependent Schrödinger equation, if the process occurs as a single quantum collision event on a rigid adiabatic PES as H_2 dissociatively sticking on metals. Otherwise calculations of the adiabatic electronic properties should be coupled with molecular dynamics simulations.

Since *ab initio* computational work is now essential in so many areas of condensed-matter science, we should like to conclude our review with some remarks on how to deal with those results. Sometimes a parallel between computer output and experimental measurements is suggested in the sense that computer output calls for interpretation (Hammer and Nørskov, 1997). While numerical results are an invaluable tool for obtaining a realistic description of complex systems such as adsorbates on metals, they cannot by themselves furnish a rational understanding of the results, and they lack predictive character. The more realistic a theoretical model becomes, the more difficult it is to identify and exhibit in the computer output those properties which determine trends from substrate to substrate for the same adsorbate or from adsorbate to adsorbate for the same substrate. This is the main motivation for simpler models such as the Anderson-Grimley-Newns model for chemisorption and adsorption on a jellium surface for physisorption. These simpler models are able to grasp general trends of the molecule-metal interaction. We also wish to point out that experimental and computer results are not parallel, because the results from experiments refer to the interaction between an observer and nature. Therefore, assuming that all experimental problems have been solved satisfactorily in measuring, for example, a binding energy and its error, that must be our reference value. While computational power allows one to include more and more aspects of a physical system, the calculation output has to be considered the result only of our picture of nature and to be taken differently from an experimental measurement. Of course the calculated and measured results have to eventually converge to the same value. Certainly in a description of, say, dissociative sticking of H_2 on a metal, an n-dimensional quantum simulation is extremely helpful. But we must be aware that all thermodynamic effects are excluded from it. Another important point concerns the code of a numerical work. In the CPU we again introduce an approximate model of the physical system. Even if intuition tells us that the more ingredients we introduce into our model and consequently into our computer program, the better the description we obtain, no guarantee exists that the almost exact solution of a model corresponds to the correct picture of the system under investigation.

ACKNOWLEDGMENTS

We are much indebted to T. B. Grimley for several enlightening comments and for a critical reading of the manuscript. We are also grateful to M. Bernasconi, V. Bortolani, P. Cortona, M. Nooijen, and G. F. Pacchioni for useful comments and discussions.

REFERENCES

Anderson, P. W., 1961, Phys. Rev. **124**, 41.
Anger, A., A. Winkler, and K. D. Rendulic, 1989, Surf. Sci. **220**, 1.
Annett, J. F., and R. Haydock, 1984, Phys. Rev. Lett. **53**, 838.
Annett, J. F., and R. Haydock, 1986, Phys. Rev. B **34**, 6860.
Bachelet, G. B., D. R. Hamann, and M. Schlüter, 1982, Phys. Rev. B **26**, 4199.
Bagus, P. S., and G. Pacchioni, 1992, Surf. Sci. **278**, 427.
Batteas, J. D., J. C. Dunphy, G. A. Somorjai, and M. Salmeron, 1996, Phys. Rev. Lett. **77**, 534.
Becke, A. D., 1988, Phys. Rev. A **38**, 3098.
Becke, A. D., 1995, in *Modern Electronic Structure Theory*, edited by D. R. Yarkony (World Scientific, Singapore), Vol. 2, p. 1022.
Benesh, G. A., and L. S. G. Liyanage, 1994, Phys. Rev. B **49**, 17264.
Bird, D. M., and P. A. Gravil, 1997, Surf. Sci. **377-379**, 555.
Bird, D. M., J. White, and P. Gravil, 1996, Gas-Surface News **15**, 6.
Bormet, J., J. Neugebauer, and M. Scheffler, 1994, Phys. Rev. B **49**, 17242.
Born, M., and K. Huang, 1954, in *Dynamical Theory of Crystal Lattices* (Oxford, Clarendon), p. 406.
Born, M., and R. Oppenheimer, 1927, Ann. Phys. (Leipzig) **84**, 457.
Bortolani, V., and A. C. Levi, 1986, Riv. Nuovo Cimento **9**, 1.
Brenig, W., and K. Schönhammer, 1974, Z. Phys. **267**, 201.
Brivio, G. P., 1987, Phys. Rev. B **35**, 5975.
Brivio, G. P., and T. B. Grimley, 1977, J. Phys. C **10**, 2351.
Brivio, G. P., and T. B. Grimley, 1983, Surf. Sci. **131**, 475.
Brivio, G. P., and T. B. Grimley, 1993, Surf. Sci. Rep. **17**, 1.
Brivio, G. P., T. B. Grimley, V. Bortolani, and G. Santoro, 1993, Chem. Phys. Lett. **208**, 93.
Bruch, L. W., M. W. Cole, and E. Zaremba, 1997, *Physical Adsorption: Forces and Phenomena* (Clarendon, Oxford).
Callaway J., 1974, *Quantum Theory of the Solid State* (Academic, San Diego/New York).
Car, R., and M. Parrinello, 1985, Phys. Rev. Lett. **55**, 2471.
Celli, V., 1984, in *Many-Body Phenomena at Surfaces*, edited by D. Langreth and H. Suhl (Academic, Orlando), p. 315.
Ceperley, D. M., 1978, Phys. Rev. B **18**, 3126.
Ceperley, D. M., and B. J. Alder, 1980, Phys. Rev. Lett. **45**, 566.

Chizmeshya, A., and E. Zaremba, 1992, Surf. Sci. **268**, 432.
Cohen, P. I., J. Unguris, and M. B. Webb, 1975, Bull. Am. Phys. Soc. **20**, 406.
Colbourn, E. A., 1992, Surf. Sci. Rep. **15**, 281.
Cole, M. W., and F. Toigo, 1985, Phys. Rev. B **31**, 727.
Cortona, P., 1986, Phys. Rev. A **34**, 769.
Cortona, P., M. G. Dondi, A. Lausi, and F. Tommasini, 1992, Surf. Sci. **276**, 333.
Cvetko, V., A. Lausi, A. Morgante, F. Tommasini, P. Cortona, and M. G. Dondi, 1994, J. Chem. Phys. **100**, 2052.
Dai, J., and J. C. Light, 1997, J. Chem. Phys. **107**, 1676.
Darling, G. R., and S. Holloway, 1994, Surf. Sci. **304**, L461.
Darling, G. R., and S. Holloway, 1995, Rep. Prog. Phys. **58**, 1595.
Dreizler, R. M., and E. K. U. Gross, 1990, *Density Functional Theory* (Springer, Berlin).
Drittler, B., M. Weinert, R. Zeller, and P. H. Dederichs, 1989, Phys. Rev. B **39**, 930.
Einstein, T. L., 1995, in *Physical Structure of Solid Surfaces*, edited by W. N. Unertl (Elsevier, Amsterdam), p. 1.
Ertl, G., 1994, Surf. Sci. **299-300**, 742.
Esbjerg, N., and J. K. Nørskov, 1980, Phys. Rev. Lett. **45**, 807.
Fahmi, A., and R. A. van Santen, 1997, Surf. Sci. **371**, 43.
Feibelman, P. J., 1990, Phys. Rev. Lett. **65**, 729.
Feibelman, P. J., 1991a, Phys. Rev. B **43**, 9452.
Feibelman, P. J., 1991b, Phys. Rev. Lett. **67**, 461.
Feibelman, P. J., 1992a, Phys. Rev. Lett. **69**, 1568.
Feibelman, P. J., 1992b, Phys. Rev. B **46**, 15416.
Fetter, A. L., and J. D. Walecka, 1971, *Quantum Theory of Many-Particle Systems* (McGraw-Hill, New York).
Filippi, C., X. Gonze, and C. J. Umrigar, 1996, in *Recent Development and Applications of Modern Density Functional Theory*, edited by J. M. Seminario (Elsevier, Amsterdam), p. 295.
Friedel, J., 1954, Adv. Phys. **3**, 446.
Galli, G., and M. Parrinello, 1991, in *Computer Similation in Materials Science*, edited by M. Meyer and V. Pontikis, NATO ASI Series E No. 205 (Kluwer Academic, Dordrecht), p. 283.
Ganduglia-Pirovano, M. V., J. Kudrnovský, and M. Scheffler, 1997, Phys. Rev. Lett. **78**, 1807.
Gomer, R., 1990, Rep. Prog. Phys. **53**, 917.
Gravil, P. A., D. M. Bird, and J. A. White, 1996, Phys. Rev. Lett. **77**, 3933.
Grimley, T. B., 1958, Proc. Phys. Soc. London, Sect. A, **72**, 103.
Grimley, T. B., 1967, Proc. Phys. Soc. London Sect. A, **90**, 751.
Grimley, T. B., 1975, Prog. Surf. Membr. Sci. **9**, 71.
Grimley, T. B., 1976, in *Electronic Structure and Reactivity of Metal Surfaces*, edited by E. G. Derouane and A. A. Lucas (Plenum, New York/London), p. 113.
Grimley, T. B., 1983, in *The Chemical Physics of Solid Surfaces and Heterogeneous Catalysis*, edited by D. A. King and D. P. Woodruff (Elsevier, Amsterdam), No. 2, p. 333.
Grimley, T. B., and C. Pisani, 1974, J. Phys. C **7**, 2831.
Gross, A., 1996, Surf. Sci. **363**, 1.
Gross, A., B. Hammer, M. Scheffler, and W. Brenig, 1994, Phys. Rev. Lett. **73**, 3121.
Gross, A., S. Wilke, and M. Scheffler, 1995, Phys. Rev. Lett. **75**, 2718.
Grunze, M., 1982, in *The Chemical Physics of Solid Surfaces and Heterogeneous Catalysis*, edited by D. A. King and D. P. Woodruff (Elsevier, Amsterdam), No. 4, p. 143.
Gunnarsson, O., and H. Hjelmberg, 1975, Phys. Scr. **11**, 97.
Gunnarsson, O., H. Hjelmberg, and B. I. Lundqvist, 1976, Phys. Rev. Lett. **37**, 292.
Gunnarsson, O., H. Hjelmberg, and B. I. Lundqvist, 1977, Surf. Sci. **63**, 348.
Gunnarsson, O., and B. I. Lundqvist, 1976, Phys. Rev. B **13**, 4274.
Gunnarsson, O., B. I. Lundqvist, and J. W. Wilkins, 1974, Phys. Rev. B **10**, 1319.
Hammer, B., K. W. Jacobsen, and J. K. Nørskov, 1992, Phys. Rev. Lett. **69**, 1971.
Hammer, B., K. W. Jacobsen, and J. K. Nørskov, 1993, Phys. Rev. Lett. **70**, 3971.
Hammer, B., Y. Morikawa, and J. K. Nørskov, 1996, Phys. Rev. Lett. **76**, 2141.
Hammer, B., and J. K. Nørskov, 1995a, Surf. Sci. **343**, 211; 1996, **359**, 306(E).
Hammer, B. and Nørskov, J. K., 1995b, Nature (London) **376**, 238.
Hammer, B., and J. K. Nørskov, 1997, in *Chemisorption and Reactivity on Supported Clusters and Thin Films*, edited by R. M. Lambert and G. Pacchioni, NATO ASI Series E No. 331 (Kluwer Academic, Dordrecht), p. 285.
Hammer, B., and M. Scheffler, 1995, Phys. Rev. Lett. **74**, 3487.
Hammer, B., M. Scheffler, K. W. Jacobsen, and J. K. Nørskov, 1994, Phys. Rev. Lett. **73**, 1400.
Hamnett, A., 1990, in *Interaction of Atoms and Molecules with Solid Surfaces*, edited by V. Bortolani, N. H. March, and M. P. Tosi (Plenum, New York/London), p. 599.
Harris, J., and A. Liebsch, 1982, J. Phys. C **15**, 2275.
Hedin, L., and B. I. Lundqvist, 1971, J. Phys. C **4**, 2064.
Hennig, D., M. V. Ganduglia-Pirovano, and M. Scheffler, 1996, Phys. Rev. B **53**, 10344.
Hermann, K., 1992, in *Cluster Models for Surface and Bulk Phenomena*, edited by G. Pacchioni, P. S. Bagus, and F. Parmigiani, NATO ASI Series B No. 283 (Plenum, New York/London), p. 209.
Hjelmberg, H., O. Gunnarsson, and B. I. Lundqvist, 1977, Surf. Sci. **68**, 158.
Hohenberg, P. and W. Kohn, 1964, Phys. Rev. **136**, B864.
Hu, P., D. A. King, S. Crampin, M. H. Lee, and M. C. Payne, 1994, Chem. Phys. Lett. **230**, 502.
Hult, E., Y. Andersson, B. I. Lundqvist, and D. C. Langreth, 1996, Phys. Rev. Lett. **77**, 2029.
Hult, E., and A. Kiejna, 1997, Surf. Sci. **383**, 88.
Inglesfield, J. E., 1981, J. Phys. C **14**, 3795.
Inglesfield, J. E., and G. A. Benesh, 1988a, Phys. Rev. B **37**, 6682.
Inglesfield, J. E., and G. A. Benesh, 1988b, Surf. Sci. **200**, 135.
Inglesfield, J. E., and B. W. Holland, 1981, in *The Chemical Physics of Solid Surfaces and Heterogeneous Catalysis*, edited by D. A. King and D. P. Woodruff (Elsevier, Amsterdam), No. 1, p. 183.
Ishida, H., 1990, Phys. Rev. B **41**, 12288.
Ishida, H., 1997, Surf. Sci. **388**, 71.
Jennison, D. R., P. A. Schultz, and M. P. Sears, 1996, Phys. Rev. Lett. **77**, 4828.
Johnson, B. G., P. M. W. Gill, and J. A. Pople, 1993, J. Chem. Phys. **98**, 5612.
Jones, R. O., and O. Gunnarsson, 1989, Rev. Mod. Phys. **61**, 689.
Karikorpi, M., M. Manninen, and C. Umrigar, 1986, Surf. Sci. **169**, 299.

Kay, M., G. R. Darling, S. Holloway, J. A. White, and D. M. Bird, 1995, Chem. Phys. Lett. **245**, 311.
Kellogg, G. L., and P. J. Feibelman, 1990, Phys. Rev. Lett. **64**, 3143.
Kohn, W., 1990, in *Interaction of Atoms and Molecules with Solid Surfaces*, edited by V. Bortolani, N. H. March, and N. P. Tosi (Plenum, New York/London), p. 53.
Kohn, W., A. D. Becke, and R. G. Parr, 1996, J. Phys. Chem. **100**, 12974.
Kohn, W., and L. J. Sham, 1965, Phys. Rev. **140**, A1133.
Kohn, W., and P. Vashishta, 1983, in *Theory of the Inhomogeneous Electron Gas*, edited by S. Lundqvist and N. H. March (Plenum, New York/London), p. 79.
Kratzer, P., B. Hammer, and J. K. Nørskov, 1996, Surf. Sci. **359**, 45.
Kroes, G. J., E. J. Baerends, and R. C. Mowrey, 1997, Phys. Rev. Lett. **78**, 3583.
Lang, N. D., 1981, Phys. Rev. Lett. **46**, 842.
Lang, N. D., and J. K. Nørskov, 1983, Phys. Rev. B **27**, 4612.
Lang, N. D., and A. R. Williams, 1975, Phys. Rev. Lett. **34**, 531.
Lang, N. D., and A. R. Williams, 1976, Phys. Rev. Lett. **37**, 212.
Lang, N. D., and A. R. Williams, 1978, Phys. Rev. B **18**, 616.
Lang, P., V. S. Stepanyuk, K. Wildberger, R. Zeller, and P. H. Dederichs, 1994, Solid State Commun. **92**, 755.
Langmuir, I., 1922, Trans. Faraday Soc. **17**, 607.
Lee, C. W. Yang, and R. G. Parr, 1988, Phys. Rev. B **37**, 785.
Levy, M., and J. P. Perdew, 1985, Phys. Rev. A **32**, 2010.
Lewis, P. S., and A. M. Rappe, 1996, Phys. Rev. Lett. **77**, 5241.
Lifshitz, E. M., 1955, Zh. Tekh. Fiz. **29**, 94.
Louie, S. G., and M. L. Cohen, 1976, Phys. Rev. B **13**, 2461.
Lundqvist, B. I., 1984, in *Many-Body Phenomena at Surfaces*, edited by D. Langreth and H. Suhl (Academic, Orlando), p. 93.
Majumdar, D., and K. Balasubramanian, 1997, J. Chem. Phys. **106**, 7215.
Manninen, M., J. K. Nørskov, M. J. Puska, and C. Umrigar, 1984, Phys. Rev. B **29**, 2314.
March, N. H., 1983, in *Theory of the Inhomogeneous Electron Gas*, edited by S. Lundqvist and N. H. March (Plenum, New York/London), p. 1.
Messmer, R. P., 1979, in *The Nature of the Surface Chemical Bond*, edited by T. N. Rhodin and G. Ertl (North-Holland, Amsterdam), p. 51.
Michelsen, H. A., and D. J. Auerbach, 1991, J. Chem. Phys. **94**, 7502.
Montalenti, F., M. I. Trioni, G. P. Brivio, and S. Crampin, 1996, Surf. Sci. **364**, L595.
Newns, D. M., 1969, Phys. Rev. **178**, 1123.
Nilsson, A., M. Weinelt, T. Wiell, P. Bennich, O. Karis, N. Wassdahl, N. Stohr, and M. G. Samant, 1997, Phys. Rev. Lett. **78**, 2847.
Nørskov, J. K., 1982, Phys. Rev. B **26**, 2875.
Nørskov, J. K., 1990, Rep. Prog. Phys. **53**, 1253.
Nørskov, J. K., and N. D. Lang, 1980, Phys. Rev. B **21**, 2131.
Pacchioni, G., 1995, Heterog. Chem. Rev. **2**, 213.
Pacchioni, G., S. C. Chung, S. Krüger, and N. Rösch, 1997, Surf. Sci. **392**, 173.
Panas, I., J. Schüle, P. E. M. Siegbahn, and U. Wahlgren, 1988, Chem. Phys. Lett. **149**, 265.
Parr, R. G., and W. Yang, 1989, *Density Functional Theory of Atoms and Molecules* (Oxford University Press, New York).
Payne, M. C., M. P. Teter, D. C. Allan, T. A. Arias, and J. D. Joannopoulos, 1992, Rev. Mod. Phys. **64**, 1045.
Perdew, J. P., 1985, Phys. Rev. Lett. **55**, 1665: 1985, **55**, 2370(E).
Perdew, J. P., 1995, in *Density Functional Theory*, edited by E. K. U. Gross and R. M. Dreizler, NATO ASI Series B No. 337 (Plenum, New York/London), p. 51.
Perdew, J. P., J. A. Chevary, S. H. Vosko, K. A. Jackson, M. R. Pederson, D. J. Singh, and C. Fiolhais, 1992, Phys. Rev. B **46**, 6671.
Perdew, J. P., and A. Zunger, 1981, Phys. Rev. B **23**, 5048.
Persson, M., and J. Harris, 1987, Surf. Sci. **187**, 67.
Petersen, M., S. Wilke, P. Ruggerone, B. Kohler, and M. Scheffler, 1996, Phys. Rev. Lett. **76**, 995.
Pisani, C., 1978, Phys. Rev. B **17**, 3143.
Press, H. W., B. P. Flannery, S. A. Teukolsky, and W. T. Vetterling, 1989, in *Numerical Recipes: The Art of Scientific Computing* (Cambridge University, Cambridge), p. 431.
Puska, M. J., R. M. Nieminen, and M. Manninen, 1981, Phys. Rev. B **24**, 3037.
Raeker, T. J., and A. E. DePristo, 1990, Surf. Sci. **235**, 84.
Rendulic, K. D., G. Anger, and A. Winkler, 1989, Surf. Sci. **208**, 404.
Rasolt, M., and D. J. W. Geldart, 1986, Phys. Rev. B **34**, 1325.
Rettner, C. T., D. J. Auerbach, and H. A. Michelsen, 1992, Phys. Rev. Lett. **68**, 2547.
Rettner, C. T., H. A. Michelsen, and D. J. Auerbach, 1995, J. Chem. Phys. **102**, 4625.
Rieder, K. H., 1994, Surf. Rev. Lett. **1**, 51.
Rieder, K. H., and N. Garcia, 1982, Phys. Rev. Lett. **49**, 43.
Rieder, K. H., N. Garcia, and V. Celli, 1981, Surf. Sci. **108**, 169.
Rieder, K. H., G. Parschau, and B. Burg, 1993, Phys. Rev. Lett. **71**, 1059.
Rieder, K. H., and W. Stocker, 1984, Phys. Rev. Lett. **52**, 352.
Robota, H. R., Vielhaber, W., M. C. Lin, J. Segner, and G. Ertl, 1985, Surf. Sci. **155**, 101.
Rodriguez, J. A., and D. W. Goodman, 1992, Science **257**, 897.
Salanon, B., 1984, J. Phys. (Paris) **45**, 1373.
Sato, S., 1955, Bull. Chem. Soc. Jpn. **28**, 450.
Sauer, J., 1989, Chem. Rev. **89**, 199.
Scheffler, M., Ch. Droste, A. Fleszar, F. Máca, G. Wachutka, and G. Barzel, 1991, Physica B **172**, 143.
Schlüter, M., J. R. Chelikowsky, S. G. Louie, and M. L. Cohen, 1975, Phys. Rev. B **12**, 4200.
Seminario, J. M., 1996, Ed., *Recent Development and Applications of Modern Density Functional Theory* (Elsevier, Amsterdam).
Siegbahn, P. E. M., M. A. Nygren, and V. Wahlgren, 1992, in *Cluster Models for Surface and Bulk Phenomena*, edited by G. Pacchioni, P. S. Bagus, and F. Parmigiani, NATO ASI Series B No. 283 (Plenum, New York/London), p. 267.
Sinfelt, J. H., 1984, in *Many-Body Phenomena at Surface*, edited by D. Langreth and H. Suhl (Academic, Orlando), p. 551.
Spanjaard, D., and M. C. Desjonquères, 1990, in *Interaction of Atoms and Molecules with Solid Surfaces*, edited by V. Bortolani, N. H. March, and N. P. Tosi (Plenum, New York/London), p. 255.
Stampfl, C., and M. Scheffler, 1997, Phys. Rev. Lett. **78**, 1500.
Stepanyuk, V. S., W. Hergert, K. Wildberger, R. Zeller, and P. H. Dederichs, 1996, Phys. Rev. B **53**, 2121.
Stich, I., R. Car, M. Parrinello, and S. Baroni, 1989, Phys. Rev. B **39**, 4997.
Stoll, H., C. M. E. Pavlidou, and H. Preuss, 1978, Theor. Chim. Acta **149**, 143.

Stott, M. J., and E. Zaremba, 1980, Phys. Rev. B **22**, 1564.
Stumpf, R., and M. Scheffler, 1996, Phys. Rev. B **53**, 4958.
Szabo, A., and N. S. Ostlund, 1982, *Modern Quantum Chemistry* (Macmillan, New York).
Tang, K. T., and J. P. Toennies, 1984, J. Chem. Phys. **80**, 3726.
Taylor, J. R., 1972, *Scattering Theory*, Chap. 8 (Wiley, New York/Toronto).
te Velde, G., and E. J. Baerends, 1993, Chem. Phys. **177**, 399.
Trioni, M. I., G. P. Brivio, S. Crampin, and J. E. Inglesfield, 1996, Phys. Rev. B **53**, 8052.
Trioni, M. I., S. Marcotulio, G. Santoro, V. Bortolani, G. Palumbo, and G. P. Brivio, 1998, Phys. Rev. B **58**, 11 045.
Trioni, M. I., F. Montalenti, and G. P. Brivio, 1998, Surf. Sci. Lett. **401**, L383.
Trioni, M. I., G. Palumbo, and G. P. Brivio, 1999, Surf. Sci. (in press).
von Barth, U., and L. Hedin, 1972, J. Phys. C **5**, 1629.
Vosko, S. H., and L. Wilk, 1983, J. Phys. B **16**, 3687.
Vosko, S. H., L. Wilk, and M. Nusair, 1980, Can. J. Phys. **58**, 1200.
Wachutka, G., A. Fleszar, F. Máca, and M. Scheffler, 1992, J. Phys.: Condens. Matter **4**, 2831.
Wang, S. C., and G. Ehrlich, 1993, Phys. Rev. Lett. **70**, 41.
White, J. A., and D. M. Bird, 1993, Chem. Phys. Lett. **213**, 422.
White, J. A., D. M. Bird, M. C. Payne, and I. Stich, 1994, Phys. Rev. Lett. **73**, 1404.
Whitten, J. L., and H. Yang, 1996, Surf. Sci. Rep. **218**, 55.
Wiesenekker, G., G. J. Kroes, and E. J. Baerends, 1996, J. Chem. Phys. **104**, 7344.
Wilke, S., M. H. Cohen, and M. Scheffler, 1996, Phys. Rev. Lett. **77**, 1560.
Wilke, S., and M. Scheffler, 1995, Surf. Sci. Lett. **329**, L605.
Wilke, S., and M. Scheffler, 1996a, Phys. Rev. B **53**, 4926.
Wilke, S., and M. Scheffler, 1996b, Phys. Rev. Lett. **76**, 3380.
Williams, A. R., P. J. Feibelman, and N. D. Lang, 1982, Phys. Rev. B **26**, 5433.
Yang, H., and J. L. Whitten, 1993, J. Chem. Phys. **98**, 5039.
Yang, H., and J. L. Whitten, 1997, Surf. Sci. **370**, 136.
Zangwill, A., 1988, *Physics at Surfaces* (Cambridge University, Cambridge), p. 60.
Zaremba, E., and W. Kohn, 1976, Phys. Rev. B **13**, 2270.
Zaremba, E., and W. Kohn, 1977, Phys. Rev. B **15**, 1769.
Zonnevylle, M. C., J. J. C. Geerlings, and R. A. van Santen, 1994, J. Catal. **148**, 417.